Bulletin of the Seismological Society of America. Vol. 62, No. 6, pp. 1711–1751. December 1972

SEISMICITY AND TECTONICS OF WESTERN VENEZUELA

BY JAMES W. DEWEY

ABSTRACT

New seismicity data on western Venezuela and northeastern Colombia are presented. Teleseismically recorded earthquakes from 1930 through 1970 have been relocated by Joint Hypocenter Determination (JHD) or with source-station adjustments calculated by JHD. Additionally, 540 days of recording have been obtained with local seismographs installed near the Boconó Fault.

The most intense shallow activity occurred north and south of the Tachira Depression along the eastern flank of the Cordillera Oriental of Colombia. The Boconó Fault Zone is seismically active; small shallow shocks were recorded in it by the local stations. Shallow earthquakes also occur in the Cordillera de Mérida away from the Boconó Fault.

The new hypocenters for the intermediate-depth Bucaramanga earthquakes define a smaller source volume than defined by previously computed hypocenters. A previously inferred southward-dipping seismic zone near Bucaramanga is probably spurious, a consequence of correlation between errors in latitude and errors in depth. If one assumes that these intermediate-depth earthquakes lie on a single lithospheric slab, that slab strikes approximately north and dips to the east.

The distribution of hypocenters and focal mechanisms support the plate-tectonic hypothesis that the present tectonics of northwestern Venezuela are a result of eastward motion of the Caribbean plate with respect to the South American plate. The principal interface between these two plates may have changed within the last 5 m.y. from a zone of underthrusting west of the Sierra de Perija to the predominantly right-lateral Boconó Fault Zone.

INTRODUCTION

This paper presents new seismicity data on western Venezuela and northeastern Colombia in the area bounded by 6°N to 13°N latitude and 68°W to 74°W longitude. The region considered lies between the Precambrian Guayana Shield and the basins of the Caribbean Sea, and includes the northeastern termination of the Andes Mountains (Figure 1). Despite several analyses of the region in terms of the theory of global plate tectonics, there is still no agreement as to even the general characteristics of the present-day tectonics of the region. For example, Molnar and Sykes (1969) and Case *et al.* (1971) consider the tectonics of the region to be a consequence of the motion of the Caribbean (or Caribbean-Nazca) plate eastward, or northeastward, with respect to the South American plate (Figure 2), whereas Freeland and Dietz (1971) consider the Caribbean plate to be presently attached to the South American plate, with little or no relative motion between the two.

The Boconó Fault Zone is a major strike-slip fault zone showing many superficial similarities to the San Andreas Fault Zone of California (Rod, 1956). Short-period vertical seismographs installed in February, 1969 in the Boconó Fault Zone have given, through November, 1970, 540 days of local recording. These are the first seismographs to record for longer than a few days in the Cordillera de Mérida.

* Present address: NOAA/ERL/ESL, Seismological Research Group, Boulder, Colorado 80302.

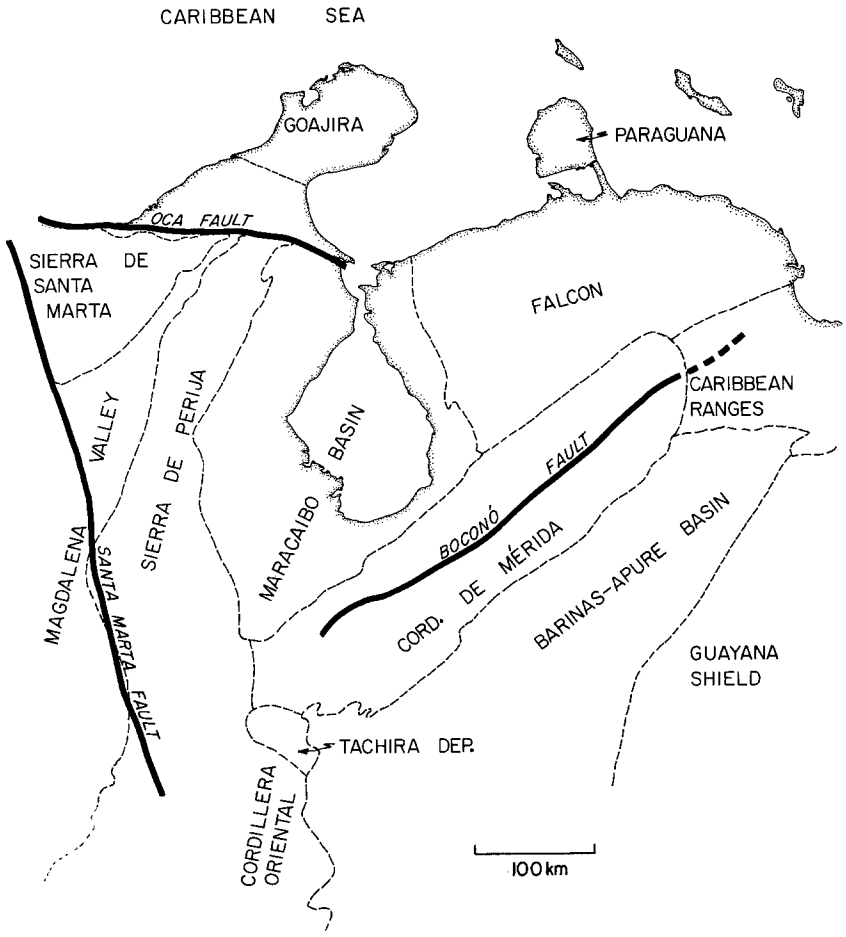

FIG. 1. Structural provinces of northwestern Venezuela (after Mencher, 1963) and adjoining northeastern Colombia.

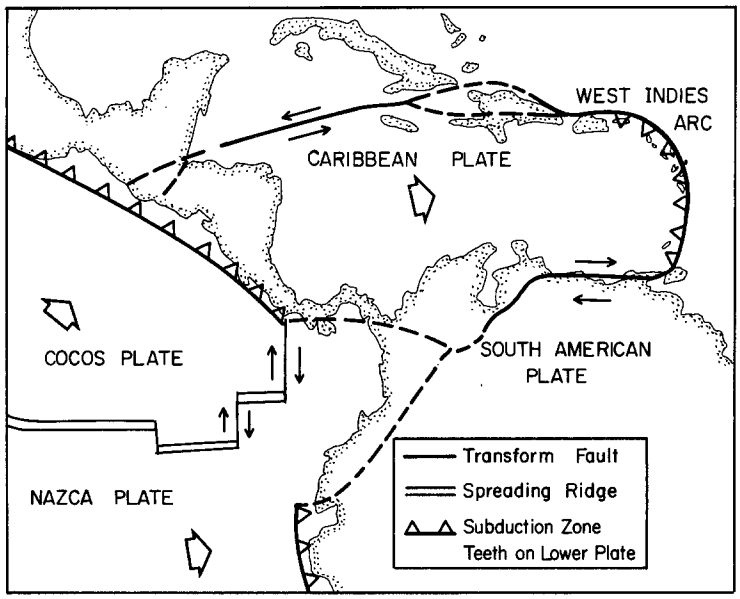

FIG. 2. Interpretation of the plate-tectonics of the Caribbean and Central American region after Molnar and Sykes (1969). Details in northern South America are from Case *et al.* (1971) and this paper.

Earthquakes with P arrival times reported from 10 or more seismographic stations from 1930 through 1970 have been relocated by the method of Joint Hypocenter Determination (JHD), or by the standard single-event method (Bolt, 1960) with travel times adjusted by the source-station adjustments calculated by JHD. Focal mechanisms of some of the more clearly recorded earthquakes have been determined using primarily P-wave first motions recorded on the short-period instruments of the World Wide Standard Seismograph Network.

Joint Hypocenter Determination (JHD)

Joint, or group determination of epicenters or hypocenters was proposed, in different forms, by Freedman (1967) and Douglas (1967) in order to minimize the effects of travel-time anomalies on the determination of the location of earthquakes and explosions. A modification of Douglas' method has been adopted. It has been tested on sources with known epicenters (Dewey, 1971).

Consider a group of K earthquakes and J recording stations. We are given a set of tables listing P-wave travel times as a function of distance and depth, and we are given provisional hypocenters and origin times of the earthquakes. Assume that P and pP waves from all K earthquakes are delayed by the same amount, Γ_j, in transit to the jth station.

Define:

δt_k = change in origin time of kth earthquake

δx_k = change in longitude (positive east) of kth earthquake

δy_k = change in latitude (positive north) of kth earthquake

δz_k = change in depth (positive down) of kth earthquake

Az_{jk} = azimuth from kth earthquake to jth station (measured clockwise from north)

$\left(\frac{\partial T_P}{\partial \Delta}\right)_{d(j,\,k)}$ = P-wave slowness for jth station and kth provisional hypocenter, from P travel-time tables

$\left(\frac{\partial T_P}{\partial h}\right)_{d(j,\,k)}$ = change in tabulated travel time with depth for jth station and kth provisional hypocenter

$\left(\frac{\partial T_{pP-P}}{\partial h}\right)_{d(j,\,k)}$ = change with depth of tabulated $pP-P$ time interval for jth station and kth provisional hypocenter

δg_j = correction to a provisional source-station adjustment g_j, which is an estimate of the source-station anomaly Γ_j.

r_{jk} = residual, observed P-wave arrival time at jth station from kth earthquake minus P-wave arrival time calculated from provisional hypocenter, origin time, tabulated P tables, provisional station adjustment, and including correction for ellipticity of the Earth

s_{jk} = residual, observed $pP-P$ time interval for jth station and kth earthquake minus calculated $pP-P$ time appropriate to provisional hypocenter of kth earthquake

ε_{jk} = reading error or timing error at jth station for P wave from kth earthquake

ε'_{jk} = reading error or timing error at jth station for pP-wave from kth earthquake.

Assume that the location of one event in the group of K earthquakes or explosions is known *a priori*. Let the known hypocenter be that of event 1. Event 1 is here called the calibration event, and its hypocenter will be restrained to its known location. Define w_{jk}

as the weight to be applied to the jk observation. w_{jk} is set equal to zero if there is no jk observation. The first-order equations of condition in δt_k, δx_k, δy_k, δz_k, and δg_j are

$$w_{jk}\,\delta t_k - w_{jk}(\delta x_k \sin Az_{jk} + \delta y_k \cos Az_{jk})\left(\frac{\partial T_P}{\partial \Delta}\right)_{d(j,\,k)} +$$

$$w_{jk}\,\delta z_k \left(\frac{\partial T_P}{\partial h}\right)_{d(j,\,k)} + w_{jk}\,\delta g_j + w_{jk}\,\varepsilon_{jk} = w_{jk}\,r_{jk} \tag{1a}$$

and

$$w_{jk}\,\delta z_k \left(\frac{\partial T_{pP-P}}{\partial h}\right)_{d(j,\,k)} + w_{jk}\,\varepsilon'_{jk} = w_{jk}\,s_{jk} \tag{1b}$$

for $j = 1, J$; $\quad k = 2, K$;

and

$$w_{j1}\,\delta g_j + w_{j1}\,\varepsilon_{j1} = w_{j1}\,r_{j1} \tag{1c}$$

for $j = 1, J$.

Equations (1a), (1b), and (1c) are solved for δt_k, δx_k, δy_k, δz_k ($k = 2, K$) and δg_j ($j = 1, J$) by the method of least squares. Using the revised hypocenters, origin times, and source-station adjustments, equations (1a), (1b), and (1c) are formed again and solved again by least squares.

For the first two iterations, a weighting scheme developed by Bolt (1960) is used to minimize the effects of extreme residuals. The residuals r_{jk} are weighted out according to the extent to which they deviate from the mean residual in that quadrant of the Earth's surface, with respect to earthquake k, in which the station j is located. The weighting scheme for the first two iterations is quite gentle. After two iterations, one has estimates of the sample variance of the kth earthquake, s^2_{keq}, and an estimate for the sample variance of all observations, s^2_{tot}. Define ${\sigma_0}^2$ to be equal to the value of s^2_{tot} after two iterations. The weight w_{jk} for a given iteration is then set equal to

$$w_{jk} = \left\{\frac{s^2_{tot}}{s^2_{keq}} \frac{1.0}{1+0.02 \exp\left[r^2_{jk}/2{\sigma_0}^2\right]}\right\}^{\frac{1}{2}} \tag{2}$$

where s^2_{tot} and s^2_{keq} are re-estimated prior to each iteration.

Six iterations of the joint hypocenter determination were performed for the epicenters and hypocenters reported in this paper. As an example of slow but satisfactory convergence of solutions, consider a group (group 2) of 14 shallow earthquakes from northern Venezuela. Depths of all earthquakes were restrained by pP arrival times; earthquakes for which no depth phase was read were each assigned one "dummy" pP phase corresponding to a depth of 15 km. In the sixth iteration, none of the depths changed by as much as 1 km. For 11 of the 14 earthquakes, the changes in δt_k, δx_k, δy_k satisfied the conditions $|\delta t_k| < 0.1$ sec, $|\delta x_k| < 0.01°$ longitude, $|\delta y_k| < 0.01°$ latitude. The largest changes were $\delta t_k = 0.3$ sec, $\delta x_k = -0.06°$ longitude, $\delta y_k = -0.01°$ latitude, for an earthquake whose large confidence ellipse also indicated that the P-wave data for the earthquake were not of good quality. Of 45 calculated source-station adjustments, only four were changed by more than 0.1 sec in the sixth iteration. The largest change was $\delta g_j = -0.25$ sec.

The computation of 90 per cent confidence ellipses assigned to the calculated hypocentral coordinates is based on a theory which treats the observational errors as being normally distributed (Scheffé, 1959; Flinn, 1965). In tests on sources with known epi-

centers (Dewey, 1971), the 90 per cent confidence ellipses were reliable indicators of the precision of epicentral determination when the depths of the sources were fixed, in spite of the obvious non-normality of the distribution of *P*-wave residuals. However, in *hypocentral* computations, with no *pP* readings to restrain depth calculation, examples were found where extreme residuals at crucial stations caused large changes in calculated hypocentral position with little increase in the calculated variance of *P*-wave residuals; in these cases the computed "90 per cent confidence limits" are misleadingly small.

It is well to state here the limitations of the JHD method. First, the method will be less effective according to the extent of violation of the assumption of constant source-station anomaly Γ_j (estimated by g_j) between all the earthquakes in a given group and the jth station. Second, if the calibration event is mislocated, the epicenters calculated by JHD will tend to be mislocated in the same sense. Third, while JHD minimizes the influence of systematic source-station anomalies on depth determination, it does not remove the principal difficulty met in determining depths of shallow events from *P* times alone, which is the near-constancy for such events of $(\partial T_P/\partial h)_{d(j,\,k)}$ (equation 1a) at regional and teleseismic distances.

In a study of regional seismicity, with calibration events whose locations are not known independently of teleseismic *P*-wave travel times, the use of JHD-calculated station adjustments should give improved relative hypocenter location, by adjusting travel times to individual stations so that bias introduced by the different station networks recording each event is minimized. Additionally, estimates of variance of *P*-wave residuals no longer contain contributions from velocity anomalies between source and station; the sample variance will, therefore, be a better measure of reading and timing errors (Freedman, 1967), and confidence ellipses will be more reliable indicators of relative precision of hypocenter determination. In this study, the use of JHD-calculated station adjustments has been particularly valuable in the study of the distribution of intermediate-depth earthquakes and in determining tectonic trends in regions of limited geographical extent.

Relocation of Teleseisms

Teleseisms recorded from the region 6°N to 13°N, 68°W to 74.0°W, from 1930 through 1970, have been relocated and are plotted on the map, Plate A, which is folded in the pocket on the back cover of this *Bulletin*. All earthquakes considered are listed in Appendix 1, including earthquakes whose calculated epicenters fell off the map or were too poorly located to be plotted. The teleseisms are divided into five groups, according to geographical location and time of occurrence. Groups 1 and 2 include earthquakes in the northern Cordillera de Mérida and the Falcon structural province (Figure 1). Groups 3 and 4 include earthquakes in the southern Cordillera de Mérida, the Tachira depression, and the eastern slope of the Cordillera Oriental of Colombia. Group 5 includes the intermediate-depth earthquakes of the Bucaramanga source, and all earthquakes of the Sierra de Perija, Sierra de Santa Marta, and Magdalena Valley.

From each group of earthquakes, the fifteen most widely recorded were relocated by JHD. The source-station adjustments calculated by JHD were then applied to the travel times of other earthquakes in the group, and these earthquakes were relocated by the conventional single-event location method (Bolt, 1960). For a given group of earthquakes, the weighting function used to minimize the effects of extreme residuals in the single-event location program is the same as that used in the JHD solution for that group of earthquakes. The calibration event used for both groups 1 and 2, was the earthquake of July 19, 1965, restrained to a hypocenter calculated by the single-event method without

source-station adjustments (9.20°N, 70.28°W, depth = 20 km). The epicenter was on the Boconó Fault; the *P*-wave radiation pattern of this earthquake (Appendix 2) is consistent with a source on a fault striking in the same direction as the Boconó Fault and with the same right-lateral strike-slip motion as that geologically observed on the Boconó Fault. The calibration event for group 4 was the earthquake of August 29, 1970, as located by the single-event method without source-station adjustments (7.57°N, 71.95°W), restrained to depth of 25 km, which is consistent with the *P*-wave arrival time at the station UAV, located 140 km to the northeast.

The calibration event for group 3 was the earthquake of January 27, 1970, restrained to the hypocenter calculated by JHD in group 4 (7.54°N, 71.95°W, depth 49 km). The significantly greater depth of the earthquake of January 27, 1970, relative to that of the earthquake of August 29, 1970, is indicated by the *P*-wave arrival times at UAV and suggested by the fact that the earthquake of August 29 had an associated aftershock sequence whereas the earthquake of January 27 did not.

The calibration event for group 5 was the earthquake of May 7, 1968, as located by the single-event method without source-station adjustments (6.80°N, 72.99°W, depth 162 km). The depth calculation for this earthquake was restrained by nine well-recorded *pP* phases which the author read personally. The mean of the residuals of the $pP-P$ readings with respect to the tabulated $pP-P$ time intervals for a depth of 162 km was 1.15 ± 0.35 sec, indicating that the *P*-wave arrival times at near stations made the calculated hypocenter depth less than would have been determined by use of $pP-P$ time intervals alone. The other 14 earthquakes used in the JHD for group 5 occurred very close to the calibration event. The depths of the other 14 earthquakes were determined from *P* waves alone; the depths have been corroborated by *pP* phases when these could be read (Dewey, 1971).

P-wave arrival times are taken from the *International Seismological Summary*, and its successor, the *Bulletin of the International Seismological Centre*, from the *Bulletin of the Bureau Central International Séismologique*, and from the *Earthquake Data Reports* of the United States Coast and Geodetic Survey or the National Oceanic and Atmospheric Administration. In the absence of identified *pP* phases for shallow earthquakes, a fictitious *pP* time was used in order to restrain the focal depth, when the calculated depth would otherwise be negative, or when the variance of *P* readings at regional stations was so large that the strong influence of regional stations on depth determination could not be trusted. Earthquakes in groups 1 and 2 were thus restrained by *pP* times appropriate to a depth of 15 km. Earthquakes in groups 3 and 4, and shallow earthquakes in group 5, were restrained 10 km deeper, at 25 km, because of evidence that some earthquakes in these groups occur significantly deep in the crust or uppermost mantle (see below). Because of the near linear dependence of changes in depth on changes in origin time for shallow earthquakes, the effect of restraining the depth of a shallow earthquake to a slightly incorrect value appears principally in an incorrect origin time for the earthquake and much less in the earthquake's epicenter or in station adjustments calculated by JHD. Depths of earthquakes which are restrained by fictitious *pP* times are listed "N" in Appendix 1.

The "1968 Seismological Tables for *P* Phases" (Herrin *et al.*, 1968) were used as reference travel-time tables.

Registration of Local Earthquakes in the Cordillera de Mérida

In 1969, three seismographic stations were installed in western Venezuela, in a joint investigation by the University of California Seismographic Station and the Instituto

Sismológico of Caracas. These stations were the first to be operated in western Venezuela for longer than a few days. Two seismographs were installed by the University of California in the Cordillera de Mérida of the Venezuelan Andes. Each Andes seismograph consists of a Geotech S13 short-period seismometer, used as a vertical sensor, whose output is passed through a preamplifier, to drive a Geotech Helicorder amplifier whose output, in turn, is recorded on heat-sensitive paper by a Helicorder. One instrument was installed in February, 1969, at a site (LCV) 8 km northeast of Mérida, Venezuela. In April, 1969, this instrument was moved to its present location in Mérida at the Universidad de los Andes (UAV). The UAV seismograph operates at a gain of 7,000 at 1 Hz, with peak magnification of 16,000 at 4.5 Hz. The other seismograph was installed at Bailadores (BLV), and operated at a peak magnification of 65,000 at 4.5 Hz. Both sites are located on alluvial or colluvial mesas in a large valley in the Cordillera de Mérida. The Instituto Sismológico installed the third station, LGN, in April, 1969, in the Maracaibo Basin.

Identified regions within the southern Cordillera de Mérida from which earthquakes were recorded at the Andes stations are shown as letters in Plate A. These epicentral regions in most cases represent earthquakes which occurred in the 190 days in 1969 and 1970 when stations at Bailadores and Mérida were both operating. Source regions of many small earthquakes recorded at Mérida could not be identified because the station at Bailadores was not operating at the times of occurrence of the earthquakes.

The seismic velocity model used to locate the small local earthquakes is as follows: the uppermost layer extends to 12 km depth and has $V_p = 5.6$ km/sec and $V_s = 3.3$ km/sec. An intermediate layer extends from 12 to 40 km and has $V_p = 6.7$ km/sec and $V_s = 3.9$ km/sec. The mantle is assumed to have $V_p = 8.0$ km/sec and $V_s = 4.7$ km/sec. This model is identical to that used at Berkeley to locate central California earthquakes, with the exception of the depth to the Mohorovičić discontinuity, which is here assumed 10 km deeper than in California, to account for a possible thickening of the crust under the Andes.

The location procedure consisted of fixing the depths of the earthquakes, calculating origin times from UAV or BLV $S-P$ time differences, and using arrival times at UAV and BLV to determine epicentral coordinates. By analogy with central California, it was assumed for the purpose of location of small local earthquakes that the earthquakes occurred in the upper 15 km of the crust, and 0 and 15 km used as two depths to which the hypocenter is fixed. Earthquakes from most of the local source regions plotted in Plate A have signatures of relatively shallow earthquakes, with phases which appear to be crustal phases (e.g., Figures 3, 4, and 5). The notable exception was the magnitude 5.7 earthquake of January 27, 1970 (source region "A"), which was located significantly deep in the crust or uppermost mantle.

For none of the local earthquakes plotted in Plate A did the 15-km difference in assumed source depth make more than a 10-km change in the epicenter location. The letters plotted in Plate A are centered at the mean position of epicenters calculated assuming depths of 0 and 15 km. For earthquakes whose epicenters thus calculated fell significantly off the Boconó Fault Zone, alternative solutions were computed, assuming a depth of 30 km. These alternative solutions also lay significantly away from the surface trace of the fault zone. In the cases of small earthquakes lying off the fault zone, two distinct epicenters are consistent with the P-wave arrival times at BLV and UAV. The most likely of the two epicentral regions is plotted in Plate A. In the case of epicentral region "B", the choice between the two epicentral regions was made on the basis of the historical seismic inactivity of the Maracaibo Basin. In the case of epicentral region "E", the choice between the two epicenters was made on the basis of an earthquake, appar-

ently from the same source region, which was recorded while the Mérida seismograph was located at LCV. There were, thus, effectively, three stations for the determination of this epicentral region. Source region "F" was well determined by a reading at LGN for one of the earthquakes in the source area.

Magnitudes of local earthquakes were assigned by reducing the recorded amplitudes to the amplitudes which would have been recorded by an instrument with the magnification of a Wood-Anderson standard torsion seismometer. The reduced amplitudes were used, as if they had been recorded by a Wood-Anderson seismometer, with a nomogram based on Table 22.1 of Richter (1958) to determine a magnitude.

Because the seismographs were vertical-motion instruments with different response characteristics than the horizontal torsion seismographs, used in perhaps a different geological setting than that in southern California, the assigned magnitudes may be inconsistent with other magnitude scales. From conversations with Peace Corps volunteers stationed in Santa Cruz de Mora, in source region C (Plate A), it was learned that an earthquake at 0200 GMT, March 30, 1969, to which magnitude 2.3 had been assigned, was felt in a local theater as a sharp jolt which caused some people to leave the theater. The intensity implied by this felt report suggests that the magnitudes calculated in this study correspond to a higher intensity in the meizoseismal area than is usually the case for local magnitudes and intensities in California (Richter, 1958). Rather than being attributable to inconsistent magnitude calculations, however, the unexpectedly high intensity of this earthquake may be a consequence of conditions in the epicentral region more favorable to the feeling of small magnitude earthquakes than in California: such conditions exist in parts of the eastern United States (Sbar *et al.*, 1970). For local earthquakes, magnitudes calculated for BLV and UAV nearly always agreed to within several tenths of a magnitude unit.

Shallow Seismicity

The Tachira Depression and neighboring sections of the Cordillera Oriental of Colombia. The area in Plate A with the most intense shallow earthquake activity in the period 1930 to 1970 has been the eastern flank of the Cordillera Oriental of Colombia, north and south of the Tachira Depression, where the trend of the Cordillera de Mérida intersects the Cordillera Oriental (Figure 1). This region had also experienced many destructive earthquakes prior to 1930 (Ramirez, 1933; Centeno-Grau, 1940). The following tectonic characteristics are suggested by the seismicity and by the *P*-wave radiation pattern of selected earthquakes:

1. The seismicity near 7.0°N, 72.0°W is associated with a northeast-trending fault system, defined by the aftershock sequence of the earthquake of April 21, 1957 and by the northeast-trending nodal plane of the *P*-wave radiation pattern of the earthquake of December 21, 1967 (Appendix 2). The focal mechanism of the December 21, 1967, earthquake is interpreted to represent right-lateral faulting along the northeast-trending fault; this interpretation depends heavily on the dilatation read at the station BNG and reported in the USCGS *Earthquake Data Reports*. Without the BNG datum, the *P*-wave pattern could be interpreted as having been due to a northeast-trending thrust fault. The earthquakes which define the fault zone are plotted in Figure 3. The first motions listed in the ISS for the earthquake of April 21, 1957 are inconsistent among themselves, and are not an adequate test of the focal mechanism along the inferred fault.

2. The focal mechanism solution for the earthquake of January 27, 1970 (7.54°N, 71.95°W) indicates appreciable thrust faulting. However, the orientations of the nodal planes are poorly determined. The observed *P*-wave first motions are consistent with the

compressional stress, oriented approximately east-west, indicated by the focal mechanism of the nearby earthquake of December 21, 1967. The depth of the earthquake of January 27, 1970, was calculated to be 49 km from *P*-wave travel times alone. This depth was determined by JHD, with the earthquake of August 29, 1970 (7.57°N, 71.95°W), restrained as a calibration event with depth fixed at 25 km. *pP* phases, read from 11 WWSSN records of the earthquake of January 27, 1970, implied a focal depth of about 20 km; phases at two stations implied a depth of approximately 40 km. If the discrepancy between the depth implied by *P*-wave readings alone and that implied by the phase read as *pP* is not due to incorrect interpretation of the second phase, it may be due to restraining the depth of the August 29 shock to too great a depth. The lack of aftershocks to the January 27 shock suggests that the earthquake of January 27 was significantly deeper

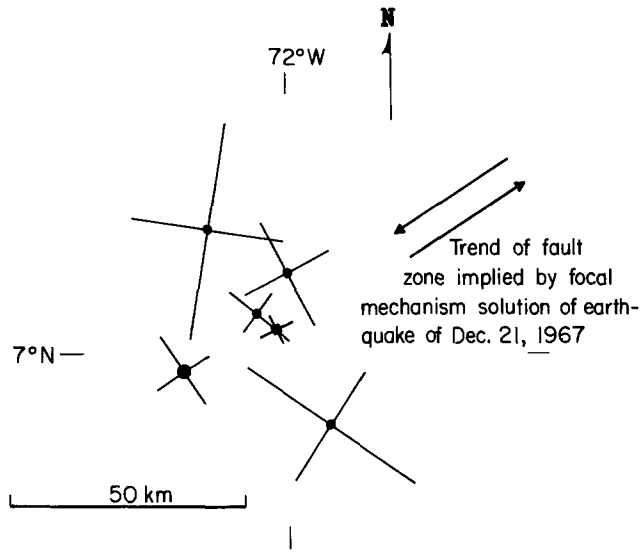

FIG. 3. Epicenters of aftershock sequence of April 21, 1957, and epicenter of earthquake of December 21, 1967, together with principal axes of 90 per cent confidence ellipses for epicenters. Large circle is main 1957 shock, small circles are 1957 aftershocks, square is 1967 shock. The epicenters with smallest confidence ellipses define a northeast trend approximately parallel to fault plane of earthquake of December 21, 1967.

than that of August 29. In the 4 days immediately following the magnitude 5.7 earthquake, not one aftershock was recorded at UAV, although aftershocks of magnitude 3.0 would have been clearly identifiable. The earthquake of August 29, magnitude 4.6, was followed by three aftershocks of magnitude greater than 3.0 in the first 4 days following the earthquake. The tendency for earthquakes in the upper crust to be followed by more aftershocks than earthquakes in the lower crust or uppermost mantle has been noted before (e.g., Page, 1968). The earthquake of April 19, 1952 (7.22°N, 72.04°W), may also have occurred in the lower crust or uppermost mantle. Thirty *pP* times were listed in the *International Seismological Summary* for this earthquake, of which 19 implied a depth greater than 33 km. The listed *pP* times show large scatter. To calculate the depth of this earthquake, one fictitious *pP* time appropriate to 50 km was used; the calculated depth of 43 km indicates that the *P* times alone would imply a depth for this earthquake of less than 50 km.

3. Taken as two responses to the same regional stress, the focal mechanisms reported in conclusions 1 and 2 indicate that the tectonics of the seismic zone from (6.8°N,

72.0°W) to (7.5°N, 72.0°W) are determined principally by a compressional stress oriented approximately east-west. The occurrence in this region of earthquakes with depths approaching 50 km also suggests that the region is one of compressive tectonics at the present time. This last inference is based on the assumption that the virtual absence of earthquakes deeper than 20 km along the very well-observed San Andreas Fault Zone in central California (Bolt *et al.*, 1968) is typical of other zones characterized by transcurrent tectonics and on the lack of any but the most shallow tectonic earthquakes reported for areas of tensional stress such as the oceanic rift systems (Isacks *et al.*, 1968).

4. South of the Tachira Depression, earthquakes with depth less than 70 km are concentrated near the eastern front of the Cordillera Oriental. From the Tachira Depression northward, the seismicity is spread over a broader area. The southern boundary of the Maracaibo Basin (Figure 1) is seismically active, and shallow earthquakes occur throughout the southern Cordillera de Mérida. The focal mechanism (Appendix 2) of the earthquake of September 2, 1964 (8.08°N, 72.78°W) indicates strike-slip motion. The trend of mapped geological faults suggests right-lateral motion along a fault striking NNE.

The Cordillera de Mérida. The Cordillera de Mérida has the general form of a broad arch in which the Eocene surface has been lifted 20,000 ft above the corresponding surface in the adjoining Barinas and Maracaibo Basins (Bucher, 1952; Rod *et al.*, 1958; Mencher, 1963). A deep central longitudinal valley, in which are located Mérida, several other towns of regional importance, and the two seismograph sites BLV and UAV, runs much of the length of the range. The valley is thought to be a consequence of faulting; in this paper, the name "Boconó Fault Zone" is applied to the fault system controlling the development of the valley, after Rod (1956).

There has been disagreement among geologists working in Venezuela as to whether the Boconó Fault Zone is a major strike-slip fault zone or a series of normal faults (Rod *et al.*, 1958). Rod (1956) first reported right-lateral strike-slip offset of Pleistocene glacial moraines in the Paramo de Muchuchies, northeast of Mérida. Schubert and Sifontes (1970) find that the average rate of right-lateral displacement along the fault in the last 10,000 years has been 0.66 cm/year. Contrasting with the evidence of recent right-lateral motion along the Boconó Fault is the evidence that motion along older, but post-Cretaceous, faults in the Boconó Fault Zone was predominantly vertical (von der Osten and Mullen in Rod *et al.*, 1958; Schubert, 1969). Mencher (1963) has suggested that the explanation for this apparent discrepancy may be that the Boconó Fault Zone originated as a series of normal faults which later coalesced into a right-lateral fault system.

The historical record (Centeno-Grau, 1940) lists many felt earthquakes for the Cordillera de Mérida: the most destructive occurred on March 26, 1812. According to the Venezuelan historian Aristides Rojas (Centeno-Grau, 1940) 500 people were killed in Mérida. Caracas, 500 km distant from Mérida, was destroyed at the same time, as were towns between Mérida and Caracas. The earthquake of April 28, 1894, was ruinous in the central longitudinal valley between Mérida and Bailadores; 319 people were killed.

We may draw the following conclusions from this study of earthquakes in the Cordillera de Mérida:

5. The Boconó Fault Zone around Mérida and between Mérida and Bailadores is seismically active. In 540 days of recording from April, 1969 through November, 1970, 13 shocks of magnitude 2.0 or greater were recorded at UAV with epicentral distances less than 24 km ($S-P \leqq 3.0$ sec). Four of these occurred within 10 km of UAV. A sampling of seismic events from within 24 km of Mérida is given in Figure 4. The seismic region "D" (Plate A) was the site of a sequence of small earthquakes on August 11–12, 1970. Within 24 hr, seven earthquakes of magnitude 2.0 or greater occurred. The largest,

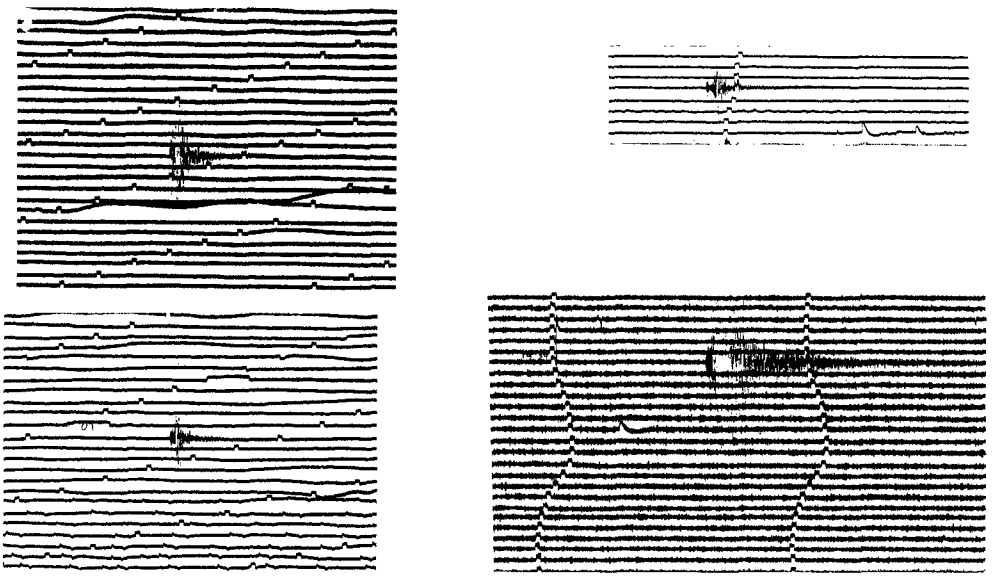

28 Dec. 1969, 2134GMT, Δ=8km, M=2.0
21 Jan. 1970, 0115 GMT, Δ=9km, M=1.8
12 Apr. 1970, 0358GMT, Δ=11km, M=1.5
31 Oct. 1970, 1938 GMT, Δ=14km, M=2.5

FIG. 4. Examples of local earthquakes occurring within 24 km of the station UAV.

magnitude 2.9, occurred near the end of the sequence. The signatures of these earthquakes are suggestive of very shallow events, giving the appearance of being so rich in various surface waves that the identification of bodily phases after the initial *P*-phase is difficult (Figure 5).

Seven earthquakes of magnitude greater than 2.0 were identified from source region "C" in 1969 and 1970, during the 190 days when BLV and UAV were both operating; the largest had magnitude 3.6. The signatures of these earthquakes, which show phases which are probably crustal phases, also appear to indicate a shallow depth of focus (Figure 6). The seismic region "H", near the village of Santo Domingo, was the site of 5 days of recording with the UAV seismograph in February, 1971, during which three

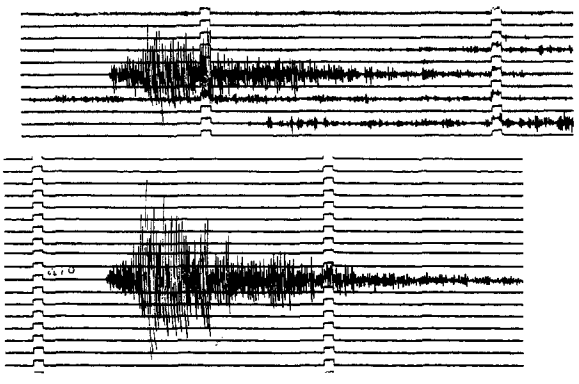

11 August 1970, 1708GMT, Δ=50km, M=2.3
12 August 1970, 0609GMT, Δ=50km, M=2.6

FIG. 5. Examples of earthquakes from source region D recorded at BLV.

earthquakes of magnitude 0.7 to 1.3 were recorded within 24 km of the recording site. Larger earthquakes, with magnitudes as high as 3.6, may have originated from source region "H" in 1969 and 1970; unfortunately, with travel times only at UAV and BLV, control of the epicentral location in the northwest-southeast direction is difficult for region "H", and the larger earthquakes may have occurred off the fault.

6. The region near the southern end of the Boconó Fault Zone, in the vicinity of BLV and source region "C", seems to be a region where large earthquakes occur more frequently than elsewhere along the Boconó Fault Zone. Since 1930, three earthquakes of magnitude 6.0 or greater have occurred in this area; the magnitude $6\frac{3}{4}$ earthquake of March 14, 1932 (8.29°N, 71.88°W), the magnitude 6 earthquake of November 4, 1933 (8.36°N, 71.81°W), and the magnitude 6 earthquake of April 6, 1945 (8.32°N, 71.15°W). In addition, the earthquake of April 28, 1894, was most violent near the source region

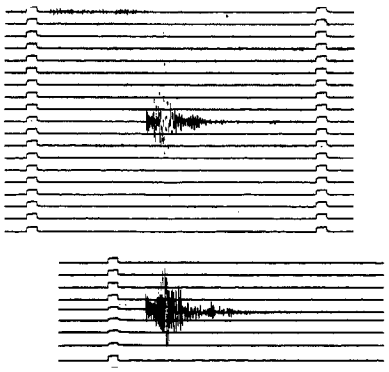

19 July 1970, 0203 GMT, Δ=20km, M=1.6
29 July 1970, 0533 GMT, Δ=22km, M=1.4

FIG. 6. Examples of earthquakes from source region C recorded at BLV.

"C" (Fiedler, 1961). Allen (1968) has noted that extremities of the Alpine Fault System of New Zealand, the San Andreas Fault System of California, and the North Anatolian Fault are characterized by the occurrence of relatively frequent large, but not great, earthquakes, and he suggests that regions where large fault systems splay out into subparallel fault systems may generally be expected to show this seismic behavior. The seismicity of the southern end of the Boconó Fault System is consistent with Allen's suggestion.

7. The first-motion pattern of the earthquake of July 19, 1965 (9.20°N, 70.28°W) is consistent with right-lateral motion along the Boconó Fault. The interpretation is strongly influenced by a dilatation read at TUC which is used to define the position of the nodal plane striking northwest. Neglecting the TUC reading, one could fit to the data a reverse fault striking due north and dipping 45° either east or west. In any case, the *P*-wave first motions cannot be interpreted in terms of normal faulting, as would be expected if the central longitudinal valley in this area were a graben (Bucher, 1952). My calculated epicenter for the El Tocuyo earthquake of August 3, 1950 (9.74°N, 69.83°W, $M = 6\frac{1}{4}$) lies off the Boconó Fault, near the town of El Tocuyo, which was strongly damaged by the earthquake. A focus on the Boconó Fault would lie within the 90 per cent confidence ellipse calculated for my epicenter. However, Von der Osten (Rod *et al.*, 1958), who did field work in the El Tocuyo area in the 1950's, felt that macroseismic effects justified an epicenter to the northwest of the main Boconó Fault.

8. Significant earthquake activity occurs in the Cordillera de Mérida away from the Boconó Fault Zone. The earthquake of May 13, 1968 (9.00°N, 71.06°W) had a focal mechanism solution (Appendix 2) with a large component of reverse faulting. The orientations of the nodal planes are not well-determined; however, all possible orientations consistent with the observed *P*-wave first motions indicate a principal compressive stress axis striking west or west-northwest. The source region "F" has been the site of three earthquakes of magnitude greater than 3.0, the largest having magnitude 3.4. A magnitude 3.3 earthquake from source region "F" was followed by four aftershocks, which suggest a relatively shallow depth of focus for the source region. The group of epicenters near 9.0°N, 69.8°W includes the epicenter of the magnitude 4.1 earthquake of January 1, 1970, which was followed by aftershocks of magnitude 2.7 and 3.0, recorded at UAV. The isolated epicenter of the magnitude $6\frac{1}{4}$ earthquake of May 1, 1931 (8.10°N, 69.64°W) is well enough determined that there can be little doubt that it occurred in the Barinas-Apure Basin at a significant distance from the Andes.

The Falcon province, the Sierra de Perija, and the adjoining portion of the continental shelf. Continuing with conclusions on the shallow seismicity of northwestern Venezuela:

9. The epicenters near 11°N, 69° to 70°W suggest an east-west zone of seismic activity distinct from the Boconó Fault System. The pattern of observed *P*-wave first motions from the magnitude 5.1 earthquake of May 19, 1970 (10.89°N, 68.93°W) (Appendix 2) is consistent with substantial right-lateral faulting parallel to the zone of epicenters, but does not require such faulting. A component of normal faulting is also present. The town of Churuguara (10.82°N, 69.53°W) has a history of small and moderate shocks (Centeno-Grau, 1940).

10. The Oca Fault Zone (Figure 1) east of 74°W is significantly less seismic than the Cordillera de Mérida and Cordillera Oriental south of Lake Maracaibo. This conclusion is suggested by the seismic activity since 1930, and is supported by the lack of great earthquakes in the recorded history of Maracaibo, settled in 1571 (Centeno-Grau, 1940).

It is possible, however, that the complete absence of calculated epicenters on the Oca Fault since 1930 is the result of bias in calculated epicenters. A pair of earthquakes on October 20, 1969, with magnitudes 5.1 and 5.7, were calculated to lie 30 km south of the Oca Fault at (10.90°N, 72.30°W) and (10.93°N, 72.46°W), respectively.

If we accept the plate-tectonic model outlined below, ray paths from earthquakes on the Oca Fault to stations in Andean South America would pass through a high-velocity slab of material in which the intermediate-depth earthquakes of northeastern Colombia are located. The early arrival of *P*-waves at stations to the south will cause a systematic shift of calculated epicenters to the south. We must consider the possibility, therefore, that the earthquakes of October 20, 1969, actually occurred on the Oca Fault.

11. The epicenters of the earthquakes occurring near 13°N, 71°W could not be located accurately enough to define a tectonic trend. These earthquakes occurred from December 21, 1943 through January 5, 1944. Gutenberg and Richter (1954) assigned magnitudes of from $6\frac{1}{4}$ to $6\frac{1}{2}$ to five of these earthquakes.

Intermediate-Depth Seismicity

Intermediate-depth earthquakes, of depths between 70 and 300 km, occur beneath the Cordillera Oriental of Colombia and the Sierra de Perija. There are no reliable hypocenters of depth greater than 70 km beneath the Cordillera de Mérida. Several of the less widely recorded earthquakes in the Cordillera de Mérida, when located without a constraint on the depth calculation, such as a *pP* reading, had calculated depths of greater than 70 km. However, the signatures of these earthquakes at the near stations

BOG and CAR suggested shallow-focus earthquakes. Moreover, the variances of *P*-wave travel-time residuals were not significantly increased by restraining the hypocenters to shallower depths of focus with the use of fictitious *pP* times.

The Bucaramanga Source of Intermediate-Depth Earthquakes

The intermediate-depth seismic zone beneath the northern Cordillera Oriental of Colombia and the Sierra de Perija includes a remarkable concentration of hypocenters beneath Bucaramanga, Colombia, which shall here be called the "Bucaramanga source". North-south and east-west sections through the Bucaramanga source are shown in Figures 7 and 8, with only A-quality hypocenters plotted. To illustrate the effect of using travel-time adjustments, the hypocenters of the same earthquakes as determined using unadjusted *P* times with the single-event location method by the International Seismological Centre or by the U.S. Coast and Geodetic Survey (now by the National Oceanic and Atmospheric Administration) are also plotted. The JHD and the single-event location method with jointly determined source-station adjustments make an appreciable reduction in the apparent volume of the Bucaramanga source. The absolute location of the source region is uncertain because the position of the calibration event used in JHD, the earthquake of May 7, 1968, was calculated by the single-event method, and may be subject to location bias. Given that the calibration event is located at 6.80°N, 72.99°W, depth 162 km, the large majority of the earthquakes from the Bucaramanga source occur in the region within latitudes 6.75°N and 6.85°N, longitudes 72.97°W and 73.07°W, and depths 158 km and 173 km. For many of the hypocenters ("A" quality and poorer), located outside the source volume where the hypocenters are densest, the 90 per cent confidence ellipsoids of the hypocenters cover portions of that source volume.

Consider the apparent southerly dip of the zone of intense activity in Figure 7 defined by the hypocenters determined with adjusted *P* times. For all of the hypocenters in the dipping zone lying north of 6.85°N or south of 6.75°N, the joint marginal confidence ellipse of latitude versus depth has the major axis dipping parallel to the zone of hypocenters. Examples of such hypocenters, which I believe are mislocated, are given in Figure 9, together with the axes of their joint marginal confidence ellipses for latitude versus depth. In other words, even for a point source of earthquakes in the Bucaramanga region, random errors in *P*-wave travel times would produce a spurious southward-dipping zone of hypocenters. The correlation of errors in latitude with errors in depth, which produces the spurious southward dip, is a consequence of the distribution of recording seismograph stations with respect to the source-region of the earthquakes and occurs whether or not the travel-times are affected by velocity anomalies. Figure 7 suggests that the spurious dip is exaggerated by the presence of velocity anomalies, however. The spurious dip is also probably exaggerated by the presence of extreme residuals, not accounted for in the derivation of the 90 per cent confidence ellipse. Such a residual at a crucial station will cause the calculated hypocenter to be severely mislocated in a direction parallel to the semi-major axis of the confidence ellipse: because the effect of the extreme residual at a crucial station is "absorbed" in mislocation of the hypocenter, rather than appearing in the estimated variance of the *P*-wave travel-times, the error in the calculated hypocenter is not "detected" by the 90 per cent confidence ellipse.

In summary, the recalculated hypocenters and their joint marginal confidence ellipses support the hypothesis (Tryggvason and Lawson, 1970) that the Bucaramanga source is a relatively small volume with radius less than 10 km. The new hypocenters and confidence ellipses do not support the hypothesis that the Bucaramanga source lies in a

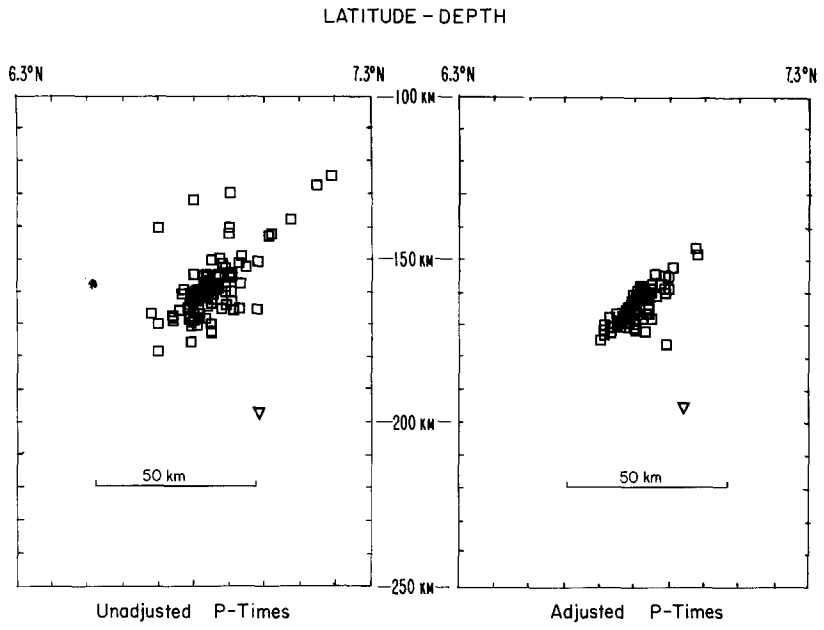

FIG. 7. North-south section through the Bucaramanga source. The triangle denotes the hypocenter of the earthquake of December 28, 1967. "Unadjusted *P*-times" hypocenters are those of the International Seismological Centre or, when ISC hypocenters are not available and after July, 1967, preliminary hypocenters of the U.S. Coast and Geodetic Survey or the National Oceanic and Atmospheric Administration. "Unadjusted *P*-times" hypocenters are plotted only for those earthquakes for which "adjusted *P*-times" hypocenters are plotted.

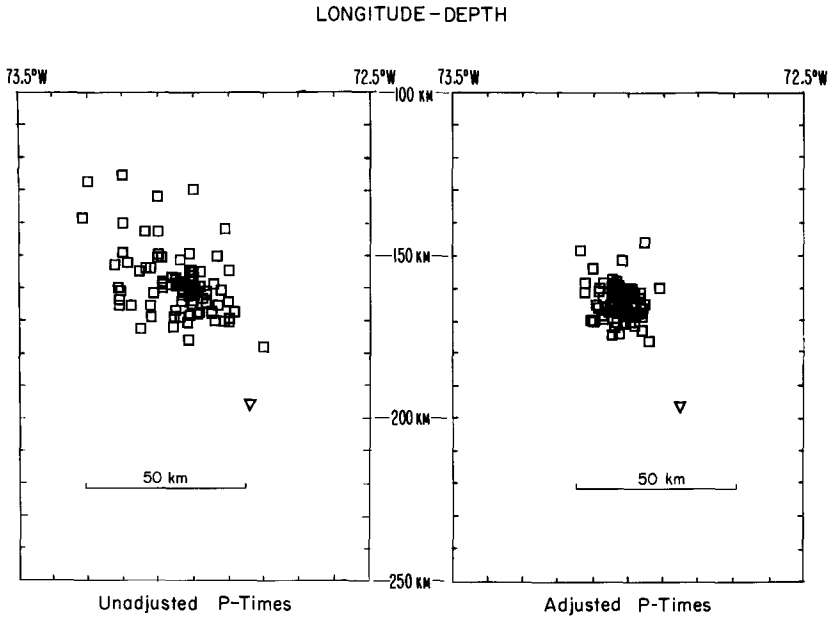

FIG. 8. East-west section through the Bucaramanga source. The triangle denotes the hypocenter of the earthquake of December 28, 1967.

southward-dipping seismic zone (Santo, 1969) as is suggested by the distribution of hypocenters published by the International Seismological Centre and U.S. Coast and Geodetic Survey, which are calculated by the single-event location method. For the purpose of defining a lithospheric slab, the dense concentration of hypocenters within the Bucaramanga source can be considered as essentially one point in the slab. Another single point of such a lithospheric slab would be the well-determined hypocenter of the earthquake of December 28, 1967 (6.95°N, 72.85°W, depth 196 km) which lies northeast of, and deeper than, the Bucaramanga source. Well-recorded *pP* phases confirm the significantly greater depth of this earthquake relative to the Bucaramanga source.

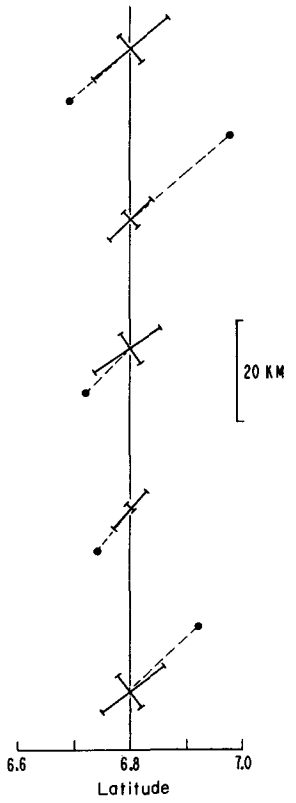

FIG. 9. Examples of the principal axes of joint marginal confidence ellipses for latitude depth for A quality hypocenters which lie outside the range (6.75°N, 6.85°N). The principal axes of each confidence ellipse are centered on 6.80°N, depth 165 km.

INTERMEDIATE-DEPTH EARTHQUAKES OCCURRING OUTSIDE THE BUCARAMANGA SOURCE

Well-located intermediate-depth earthquakes occur beneath the Cordillera Oriental and Sierra de Perija outside the Bucaramanga source. Evidence from seismicity for a continuous thin sinking slab of lithosphere beneath northeastern Colombia is not as compelling as evidence for such slabs beneath some island arc regions, because the intermediate-depth hypocenters outside of the Bucaramanga source are not numerous enough to unambiguously "require" a continuous slab.

If these earthquakes do occur in the same lithospheric slab as that containing the Bucaramanga earthquakes, that slab must have an approximately northerly strike to 10°N and dip to the east. This conclusion is consistent with the depths of the hypocenters

north of the Bucaramanga source (Plate A) and also with the position of the earthquake of December 28, 1967 with respect to the Bucaramanga source. North of 10°N, the orientation of the slab is not well-defined by the hypocenters, possibly a consequence of poor depth control in this region which is distant from a first class seismographic station. Assuming that the slab strikes due north at the location of the Bucaramanga nest, the slab has a dip there of approximately 60° to the east (Figure 8).

Some of the intermediate-depth earthquakes occurring outside the Bucaramanga nest are as large as the largest of the Bucaramanga earthquakes, but their hypocenters are isolated, rather than occurring in clusters. For example, the earthquake of June 19, 1961 (8.92°N, 73.44°W, depth 120 km) was assigned $m_b = 6.0$ (CGS), and the earthquake of November 17, 1968 (9.55°N, 72.60°W, depth 175 km) was assigned $m_b = 5.7$ (CGS), yet the hypocenter of neither earthquake is located within 40 km of any other hypocenter that I have located. If the earthquake mechanism in these earthquakes is the same as that in the Bucaramanga earthquakes, there is evidently a physical or chemical condition at the Bucaramanga nest not present in the other source regions.

Plate Tectonics of Western Venezuela

Bucher (1952) and Molnar and Sykes (1969) have suggested that the tectonics of western Venezuela are a consequence of the relative motion of the Caribbean eastward with respect to South America. In the language of global plate tectonics, the Caribbean "plate" is thought to be moving approximately eastward with respect to the South American plate (Figure 2). Farther south, the Nazca plate is also moving approximately eastward with respect to the South American plate. The seismicity of western Colombia indicates that the Nazca plate and the Caribbean plate are tectonically distinct; the manner in which the two plates interact has not been demonstrated.

The existence of a shallow seismic zone in the Cordillera de Mérida and northern Cordillera Oriental of Colombia, and the *P*-wave radiation patterns of earthquakes occurring in the shallow seismic zone, give support to the hypothesis that the Caribbean region and an adjoining portion of northwestern Venezuela and northeastern Colombia are moving eastward with respect to southern Venezuela and eastern South America. As discussed above, there were five earthquakes in the principal shallow seismic zone which were well enough recorded that characteristics of their focal mechanisms could be inferred. The short period *P*-wave radiation patterns of these earthquakes either implied reverse faulting, along planes oriented approximately north-south, or strike-slip faulting: in the latter earthquakes, one nodal plane was consistent with right-lateral faulting along planes striking east or northeast. These *P*-wave radiation patterns are those that should be expected under the general plate tectonic model of the Caribbean developed by Molnar and Sykes (1969), which was developed with independent data, without benefit of focal mechanisms of shallow earthquakes from the portions of Venezuela and Colombia considered in this paper. If the shallow earthquakes in western Venezuela are indeed the result of interaction between lithospheric plates, the seismological data reject the hypothesis that there is presently no relative motion between the Caribbean plate and the South American plate (Freeland and Dietz, 1971).

Before proceeding with an interpretation of the tectonics of western Venezuela in terms of interacting lithospheric plates, however, I must emphasize that the seismological data presented in this paper do not *require* that the plate tectonic hypothesis be valid for western Venezuela. Specifically, any alternate tectonic hypothesis which requires that the Cordillera de Mérida and the northern Cordillera Oriental of Colombia be under compressive stress, oriented approximately east-west, is also consistent with the seismological

data. The attractiveness of interpreting the present tectonics of western Venezuela in terms of interacting plates is that the characteristics of the seismicity follow as a rather direct consequence of the independently derived model of Molnar and Sykes (1969) for the whole Caribbean region, without requiring that the characteristics of plate-plate interactions in western Venezuela be significantly different than plate-plate interactions in other continental areas of the world.

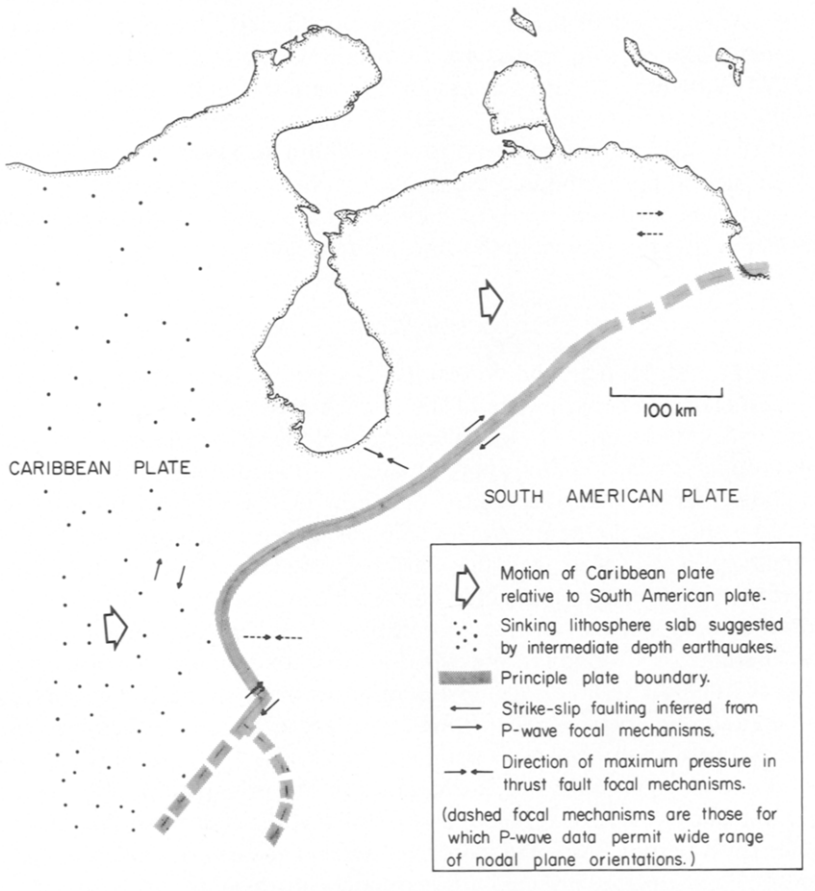

FIG. 10. Present plate boundaries in western Venezuela and northeastern Colombia.

The plate-tectonic interpretation implied by the seismicity and focal mechanisms of western Venezuela and northeastern Colombia is shown in Figure 10. The interpretation has two main characteristics.

1. The principal boundary between the two plates passes north of 7.0°N, 72.0°W along the east flank of the Cordillera Oriental, thence northeast along the Boconó Fault Zone to the Caribbean Ranges. South of 7.0°N, 72.0°W, there has been little shallow seismic activity since 1930 to define the plate boundary. North of 7.5°N, 72.0°W, the seismicity is spread over a large area, and the "plates" are here being internally deformed.

In addition to the eastward drift of the Caribbean with respect to South America, there is possibly a northern drift as well. Case *et al.* (1971) suggest that relative plate motions in this region are predominantly northeast-southwest, approximately parallel to the Boconó Fault, and of right-lateral sense. The fault-planes suggested by the short-

period *P*-wave radiation patterns (Appendix 2) are not systematic enough to determine the extent of such a northward component of Caribbean plate motion with respect to the South American plate or whether such a northward component exists. The reverse-fault focal mechanism of the earthquake of May 13, 1968, which occurred on the flank of the Cordillera de Mérida a short distance from the Boconó Fault, indicates that not all relative motion between the Caribbean and South American plates is taken up by right-lateral displacement parallel to the Boconó Fault. The direction of motion of the Caribbean with respect to South America is, therefore, probably more toward the east than the N40°E strike of the Boconó Fault.

2. The intermediate-depth earthquakes are located on a lithospheric slab striking approximately north and dipping to the east. The deepest well-located earthquakes in this zone occur at a depth of approximately 200 km. Isacks *et al.* (1968) suggest that earthquakes in a given lithospheric slab occur in those portions of the slab which were subducted within approximately the last 10 m.y. The average rate of descent of that portion of the slab containing the deepest earthquakes was, therefore, about 2 cm/year over the last 10 m.y. The average rate of underthrusting along the inclined seismic zone near the surface to the west of the intermediate-depth earthquake zone would be larger than the rate of 2 cm/year estimated for the vertical component of the slab motion. We should expect a moderately high level of shallow earthquake activity to be associated with such a rate of underthrusting.

There is not, however, an obvious zone of shallow seismicity to mark the site where the lithospheric slab containing the intermediate-depth earthquakes is initially thrust into the mantle. The seismic zone of the west coast of Colombia is 450 km west of the Bucaramanga source. One may hypothesize a lithospheric slab containing the two seismic zones, dipping east at an average 20°. A major difficulty with this model is the relative seismic inactivity of that portion of Colombia between the mountains of the west coast and the Bucaramanga source. Alternatively, the lithospheric slab containing the Bucaramanga source may be a slab which is no longer tectonically coupled to the surface. I wish to consider the implications of this last hypothesis, that the present intermediate-depth seismic zone near the Colombia-Venezuelan frontier is a remnant of a lithospheric slab which once underthrust the South American plate somewhere to the west of the present Cordillera Oriental and Sierra de Perija.

The Regional Tectonics of Western Venezuela in the Last Ten Million Years

Assume an average rate of descent of 2 cm/year for the intermediate-depth earthquake zone which now extends to 200 km. The existence of earthquakes in this zone with depths of approximately 100 km suggests that substantial underthrusting at the surface was still taking place 5 m.y. ago. For some time prior to 5 m.y. ago, then, the principle motion between the Caribbean (or possibly Nazca) plate and the South American plate southward from approximately 11.5°N must have taken place as underthrusting of the Caribbean plate beneath the South American plate along the north-south trend defined by the present zone of intermediate-depth earthquakes. The lack of intermediate-depth earthquakes north of approximately 11.5°N suggests that the zone of underthrusting terminated near this latitude. The boundary of the Caribbean plate between the north end of the zone of intermediate earthquakes at 74°W and the south end of the West Indies arc (Figure 2) must have been a right-lateral transform fault zone. The Oca Fault may be a member of the old system of right-lateral faults. A schematic diagram of the tectonic situation as it might have appeared 5 m.y. ago is shown in Figure 11.

About 5 m.y. ago, the principal boundary between the Caribbean and South American plates north of 7.5°N, 72.0°W changed to its present location in the Venezuelan Andes. At this time, right-lateral motion began along the Boconó Fault. Assuming that right-lateral motion on the Boconó Fault began 5 m.y. ago, the 50-km total right-lateral displacement on the fault estimated by Van der Osten (Rod *et al.*, 1958) must have occurred at an average rate of 1 cm/year. Considering the "order of magnitude" nature of these calculations, this average rate is remarkably consistent with the average rate of 0.66 cm/year determined for the last 10,000 years by Schubert and Sifontes (1970). An age of

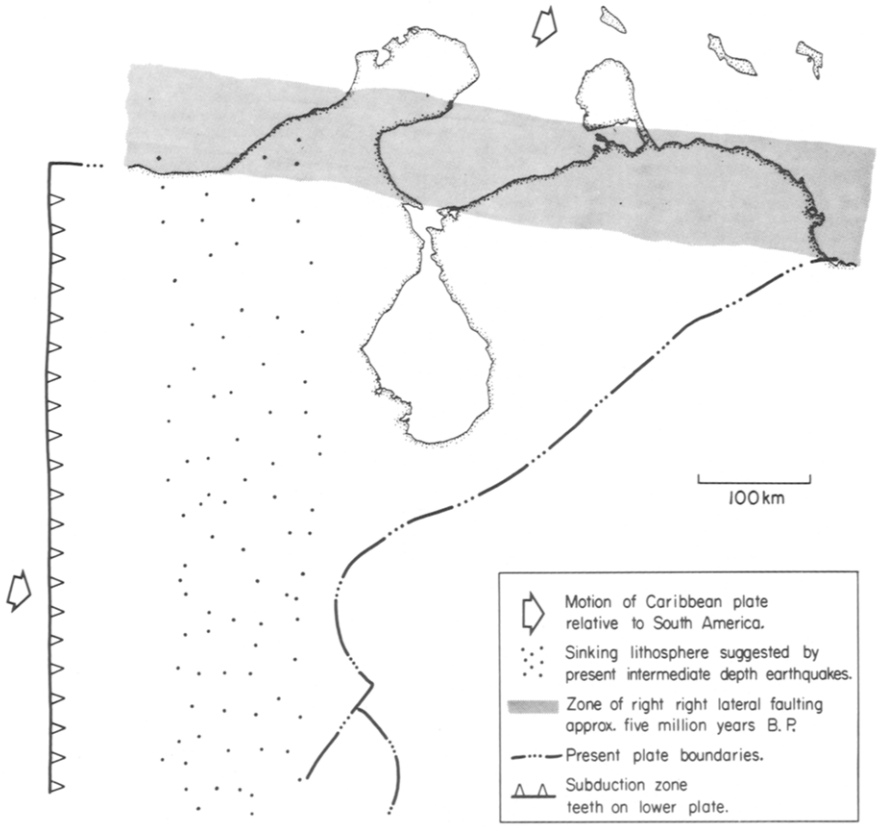

FIG. 11. Regional tectonics of western Venezuela and northeastern Colombia 5 m.y.b.p.

5 m.y. for right-lateral motion on the Boconó Fault is consistent with Mencher's (1963) view, based on the structural geology of the Cordillera de Mérida, that strike-slip motion on the fault occurred after the Eocene-Oligocene orogeny in the Cordillera. The diffuse nature of the seismicity north of 7.5°N, 72.0°W may indicate that the Earth's crust in this region is still adjusting to the change of direction of motion begun approximately 5 m.y. ago. Suppose relative motion between the Caribbean plate and the South American plate is presently occurring at the same rate of more than 2 cm/year suggested for the time period of 5 m.y. Then the 0.66 to 1 cm/year indicated for the Boconó Fault implies that more than 1 cm/year of relative motion between the two plates is taken up along tectonic features other than the Boconó Fault.

According to this speculation, the shallow seismicity south of 7.5°N must also have been concentrated west of the present Cordillera Oriental of Colombia 5 m.y. ago. The

fact that the shallow seismicity south of 7.5°N and east of 73.5°W has been concentrated on the east side of the Cordillera Oriental does not contradict this model because, in spite of the change in locus from west to east of the range, the direction of maximum compressive stress would have remained oriented east-west. North of 7.5°N, the introduction of strike-slip faulting along the Boconó Fault Zone may have changed the direction of maximum compressive stress and led to readjustments over a wide area.

Origin of the Bucaramanga Source

The remarkable clustering of earthquakes in the Bucaramanga source does not follow as a necessary consequence of the plate-tectonic model proposed above, and one must postulate complications at this portion of the descending lithospheric slab to account for the source.

The position of the Bucaramanga source is beneath a major bend of the Cordillera Oriental of Colombia, near where the Cordillera de Mérida branches at almost a right angle from the Cordillera Oriental. The character of the Bucaramanga source may be determined by the same orogenic forces which are responsible for the abrupt change of surface structural trends. Deformation of the lithospheric slab at depth may accompany the change in direction of structural features on the Earth's surface. Deformation of a sinking lithospheric slab could concentrate seismic activity in two ways: by mechanically concentrating elastic stress in a relatively small portion of the slab (Isacks and Molnar, 1971) or as a consequence of phase changes, such as melting, resulting from unusual temperature conditions associated with the change in curvature of the slab surface at the site of deformation.

At least two significantly different *P*-wave radiation patterns have been recorded from earthquakes in the Bucaramanga source. *P*-wave focal mechanism solutions for two of the largest earthquakes yet recorded from the source, the earthquakes of September 11, 1966, and July 29, 1967, are given in Appendix 2. Clearly, whatever mechanism is responsible for concentration of seismic energy release within the Bucaramanga source does not constrain shear failure to occur along a unique plane of weakness. Isacks and Molnar (1971) noted that the compressional (*P*) axes of focal mechanisms of Bucaramanga earthquakes were oriented approximately east-west; they suggested that east-west compressional stresses are dominant. Isacks and Molnar (1969) have also hypothesized that in a sinking lithospheric slab which contains intermediate-depth earthquakes, but not deep-focus earthquakes, the focal mechanisms of the intermediate-depth earthquakes should be characterized by tensional (*T*) axes directed down-dip in the slab. The focal mechanisms of the two large Bucaramanga earthquakes may be reconciled with the Isacks-Molnar hypothesis, if the seismic zone containing the Bucaramanga source locally strikes approximately N25°W and dips approximately 60°E. The tensional axes of the two large Bucaramanga shocks would then both lie in the plane of the dipping slab. The fact that the tensional axes of the two earthquakes are not parallel, then, requires that the effect of down-dip tensional stress be modified by a local condition in the lithospheric slab, such as deformation.

The focal mechanism of the intermediate-depth earthquake of November 17, 1968 (9.55°N, 72.60°W, $h = 175$ km), which occurred north of the Bucaramanga source, also has a tensional axis plunging to the east (Appendix 2). The mechanism of this earthquake, therefore, is consistent with the hypothesis that down-dip tensional stresses exert an appreciable influence on the focal mechanisms of intermediate-depth earthquakes in northeastern Colombia.

Thick Lithosphere is not Required

James (1971) has suggested that the South American lithosphere beneath the Andes of Peru, Bolivia, Argentina, and Chile is more than 200 km thick. Many intermediate-depth earthquakes with depths less than 200 km are assumed to be occurring within the stressed South American lithospheric plate, rather than in the relatively thin Nazca plate underthrusting from the west. This hypothesis of a thick South American plate is not required, however, to explain the distribution of intermediate-depth hypocenters in northeastern Colombia and northwestern Venezuela. The well-located intermediate-depth hypocenters are easily accommodated in a thin, approximately north-striking, east-dipping lithospheric slab.

Case *et al.* (1971) in their tectonic analysis of Colombia, have suggested that the Bucaramanga source region lies on the left-lateral Santa Marta Fault, which would imply again that seismic activity is taking place within or on the boundaries of a thick lithospheric slab whose upper side is still on the Earth's surface, rather than within a thin sinking lithospheric slab. The hypothesis that the Bucaramanga earthquakes occur on the Santa Marta Fault was tested with the *P*-wave radiation patterns of the Bucaramanga earthquakes and was found to be untenable. Although the Bucaramanga earthquake of September 11, 1966 had a *P*-wave radiation pattern consistent with left-lateral motion along the Santa Marta Fault (Appendix 2), focal mechanisms of other Bucaramanga earthquakes, such as that of July 29, 1967, are not consistent with such faulting.

Conclusions

The following conclusions result from this study:

1. The most intense zone of shallow activity during the interval 1930 through 1970 was in the Venezuela-Colombia border region from 6.8°N, 72.0°W, north and northwest to where the trend of the Cordillera de Mérida intersects the eastern flank of the Cordillera Oriental of Colombia. This region is under compressive tectonic stress oriented approximately east-west.

2. The Boconó Fault Zone near Mérida and between Mérida and Bailadores is seismically active; small shallow shocks were located in the fault zone during 500 days of recording with short-period seismographs in the Venezuelan Andes. The first-motion pattern of the earthquake of July 19, 1965 in the Boconó Fault Zone is consistent with right-lateral motion along the fault.

3. Significant shallow earthquake activity occurs in the Cordillera de Mérida away from the Boconó Fault Zone. The earthquake of May 13, 1968, on the flanks of the Cordillera, had a first-motion pattern indicating predominantly thrust faulting.

4. The epicenters near 11°N, 69°W to 70°W define an east-west zone of activity distinct from the Boconó fault system. The *P*-wave radiation pattern of the earthquake of May 19, 1970, is consistent with substantial right-lateral motion parallel to the zone of epicenters.

5. The recalculated hypocenters and joint marginal confidence ellipses of earthquakes from the Bucaramanga seismic source indicate that the source occupies a relatively small volume almost certainly less than 10 km in radius. The new hypocenters and confidence ellipses suggest that a previously inferred southward-dipping seismic zone in the Bucaramanga region is spurious, a consequence of a correlation between errors in latitude and errors in depth.

6. If all intermediate earthquakes in northeastern Colombia and northwestern Venezuela lie on a single continuous thin lithospheric slab, that slab strikes approximately north and dips to the east. However, the distribution of intermediate-depth

hypocenters is not dense enough to *require* that the earthquakes occur in a single lithospheric slab. There is not a continuous zone of high seismicity from the intermediate-depth earthquakes up-dip to a zone of shallow seismicity. It is, therefore, possible that the intermediate-depth earthquakes occur in a lithospheric slab which is no longer connected to surface plates.

7. An alternative hypothesis, that intermediate earthquakes occur within an unusually thick surface lithospheric plate, is not required to explain the distribution of intermediate-depth earthquakes in this portion of northern South America. The hypothesis that the Bucaramanga earthquakes occur on a deep extension of the Santa Marta Fault is not supported by the focal mechanisms of the earthquakes.

8. The characteristics of the shallow seismicity support the plate tectonic hypothesis that the present tectonics of western Venezuela are a result of continuing eastward motion of the Caribbean plate with respect to the South American plate, and argue against plate tectonic models which treat the Caribbean and South American as a single plate. The lack of shallow earthquake activity associated with the intermediate-depth earthquake zone of northern Colombia suggests that the principal boundary between the Caribbean plate and the South American plate has changed within the last 5 to 10 m.y. from a location west of the Sierra de Perija to its present position in the Cordillera de Mérida. Right-lateral strike-slip motion may have commenced on the Boconó Fault with this change in plate boundaries.

9. The use of joint hypocenter determination, or of the single-event method with source-station adjustments calculated by JHD, has proved its worth in the study of the structure of small focal regions by minimizing scatter in relative locations resulting from the use of different networks of recording stations. No teleseismically recorded earthquake was located near enough to the stations UAV and BLV to offer a definite test for systematic location bias in the Cordillera de Mérida. The application of JHD to the absolute location of shallow earthquakes in the Venezuelan Andes will become more significant as the density of local stations increases and more teleseismically recorded earthquakes can be determined locally with great precision for use as calibration events.

Acknowledgments

This paper is part of a Ph.D. dissertation (Dewey, 1971) submitted to the University of California, Berkeley. I gratefully acknowledge the encouragement and guidance of my thesis advisor, Professor Bruce A. Bolt. I received financial aid in the form of a National Defense Education Act (Title IV) Graduate Fellowship and a Fellowship from the Pan American Petroleum Foundation. The Berkeley Computer Center provided computer time for the computations.

The registration of local earthquakes in the Venezuelan Andes was part of a cooperative program with Dr. G. Fiedler and the Instituto Sismológico of Caracas, which received financial support from the Arthur L. Day Fund of the National Academy of Sciences. I enjoyed the use of facilities at the Instituto Sismológico and benefited from discussion with Dr. Fiedler.

The Ministerio de Minas e Hidrocarburos, under the directorships of A. Vivas R. and E. M. Araujo provided us with the use of the Bailadores field camp for a seismograph site.

Professor A. L. Cardenas, Director of the Centro de Ciencias at the Universidad de los Andes, arranged for the cooperation of that university with the study. Much credit for the success of the local earthquake registration must go to S. Bendayan and C. Ramirez, of the Ministerio de Minas e Hidrocarburos, and J. Cevallos C. of the Universidad de los Andes, for whose cooperation and assistance I am most grateful. I thank L. Cluff, C. Schubert, V. Winkler, and P. Villalta for discussions on problems of the Boconó Fault Zone.

I made heavy use of the WWSSN film clip library at the Earthquake Mechanism Laboratory of the National Oceanic and Atmospheric Administration, and I thank Dr. D. Tocher for this. W. Dillinger, of the Seismological Research Group, National Oceanic and Atmospheric Administration, computed focal mechanisms of the Venezuelan and Colombian earthquakes with the computer program of Dillinger *et al.* (1971).

APPENDIX 1

SEISMICITY OF THE REGION BOUNDED BY 6°N TO 13°N, 68°W TO 74°W, FROM 1930 THROUGH 1970

Earthquakes considered in this study are listed below. The following explanations apply to the listing of earthquakes:

Depth. N indicates that the depth calculation has been restrained by a fictitious *pP* time. For groups 1 and 2, the fictitious *pP* time was appropriate to a depth of 15 km. For groups 3, 4 and 5, the fictitious *pP* time was appropriate to a depth of 25 km.

The datum immediately to the right of the depth is the number of stations used in location of the earthquake by the author.

Q Quality of hypocenter determination

- A All semi-major axes of 90 per cent confidence ellipses are less than 10 km in length.
- B The largest semi-major axis of the 90 per cent confidence ellipses is greater than 10 km and less than 20 km.
- C The largest semi-major axis of the 90 per cent confidence ellipses is greater than 20 km and less than 30 km.
- D The largest semi-major axis of the 90 per cent confidence ellipses is greater than 30 km.

Only A quality epicenters are plotted for intermediate-depth earthquakes in the Bucaramanga source region in plate A. No D quality epicenters are plotted in plate A.

G J, M, and S indicate that the hypocenter was located by, respectively, JHD, the single-event method with JHD-calculated source-station adjustments, or the single-event method without source-station adjustments. The number before J or M tells which group the earthquake is in.

Mag Magnitude

- BCIS Bureau Central International Séismologique (surface-wave magnitude)
- CGS USCGS or NOS (body-wave magnitude)
- GR Gutenberg and Richter (1954) (surface-wave magnitude)
- ISC International Seismological Center (body-wave magnitude)
- PAS Pasadena (surface-wave magnitude)
- R Rothé, *The Seismicity of the Earth, 1953–1965*, UNESCO, 1969 (surface-wave magnitude)
- SE Sykes and Ewing (1965) (surface-wave magnitude)
- \+ Recorded at one of the stations BYR, CFF, HRV, KIR, MAL, MHC, PAR, PLM, RVR, SHS, SKA, STR, STU, TOL, UPP (for the earthquakes whose size is indicated by "+", a *P*-wave with trace amplitude greater than 1 mm at one of the above stations would indicate a body-wave magnitude of 5.0 or greater). On plate A, "+" earthquakes are plotted as if they were in the body-wave magnitude range 5.0 to 6.0.

For earthquakes for which surface-wave magnitudes (M_S) are listed in Appendix 1, body-wave magnitude (m_b) for use in plate A are calculated from the formula (Richter, 1958) $m_b = 2.5 + 0.63\ M_S$.

Chronological List of Earthquakes

DATE	O-TIME GMT	LAT N	LONG W	DEPTH KM	N	Q	G	MAG
1931								
MAY 01	223658.1	8.10	69.64	N	21	C	3J	6 1/4(GR)
1932								
FEB 17	160703.7	12.48	73.24	N	14	D	5M	D(GR)
MAR 14	224256.4	8.29	71.88	N	24	B	3J	6 3/4(GR)
1933								
NOV 04	084118.2	8.36	71.81	N	12	D	3J	6(GR)
1936								
NOV 23	200621.5	11.49	69.55	N	06	D	1M	+
1938								
MAY 02	234031.1	7.76	74.81	094	06	C	5M	+
1939								
AUG 11	060203.8	11.61	67.59	N	12	D	S	+
1940								
JUN 23	185935.9	10.05	68.05	N	08	D	1M	D(GR)
1941								
MAY 16	130723.1	10.81	70.07	N	09	D	1M	+
1943								
DEC 21	134621.8	12.97	71.04	N	33	C	5M	6 1/2(GR)
DEC 22	125309.2	13.19	71.02	N	32	C	5M	6 1/2(GR)
DEC 23	155605.6	12.95	71.06	N	33	C	5M	6 1/2(GR)
DEC 24	010015.5	12.92	70.95	N	26	C	5M	6 1/4(GR)
1944								
JAN 04	005757.4	13.16	71.43	N	12	C	S	+
JAN 05	105911.8	13.06	70.77	N	15	D	5M	6 1/4(GR)
1945								
APR 06	183056.5	8.32	72.15	N	15	C	4J	+
1947								
SEP 27	221244.6	8.62	71.82	N	14	C	3M	+
1948								
JAN 21	181919.3	10.24	69.85	N	15	D	1J	+
DEC 31	070802.2	8.63	71.74	N	11	C	3M	+

DATE	O-TIME GMT	LAT N	LONG W	DEPTH KM	N	Q	G	MAG
1948								
DEC 31	073122.9	8.59	71.58	N	13	C	3M	+
1950								
JUL 09	023534.2	7.79	72.59	N	29	B	3J	7.0(F)
JUL 09	032904.6	8.01	72.77	N	14	D	3M	+
JUL 09	123418.0	7.73	72.56	N	16	B	3M	+
AUG 03	092807.3	8.00	72.34	N	15	D	3M	+
AUG 03	221820.5	9.74	69.83	N	21	B	1J	6 1/4(GR)
AUG 05	104514.2	9.66	69.74	N	10	D	1M	
1951								
MAY 25	000252.4	9.71	69.76	N	15	C	1J	+
OCT 09	101311.9	10.00	69.77	N	14	D	1J	+
1952								
APR 19	095857.2	7.22	72.04	043	38	B	3J	6 3/4 - 7(PAS)
APR 19	210349.3	7.28	72.07	N	07	B	3M	
JUN 29	095640.1	8.15	72.76	157	12	C	5M	+
1954								
FEB 05	130850.5	7.20	72.13	N	13	C	3M	+
MAR 09	193906.0	7.04	73.17	183	08	C	5M	
APR 25	035708.6	8.68	72.72	N	09	C	5M	+
JUN 24	153700.7	10.86	72.15	N	07	C	5M	
JUL 25	110020.3	9.87	72.71	N	16	B	5M	4.3(SE)
SEP 17	190155.4	6.50	71.19	N	13	D	3M	+
1955								
APR 24	210800.1	6.84	72.00	N	15	B	3M	+
NOV 06	235719.9	6.78	72.51	107	13	D	3M	
1956								
JUL 03	003135.6	6.98	72.61	130	08	D	5M	
OCT 13	050442.5	9.25	69.85	N	21	C	1J	D(GR)
NOV 16	115400.1	8.20	71.23	N	29	C	3J	5.0(SE)
1957								
APR 21	211229.8	6.96	72.20	N	45	A	3J	7.1(R)
APR 22	134318.7	7.15	72.00	N	21	B	3J	+
APR 22	153725.9	7.07	72.06	N	21	A	3J	+
APR 23	175722.5	6.86	71.92	N	12	C	3M	+
APR 26	022929.8	7.23	72.15	N	12	C	3M	+
SEP 07	011036.1	8.24	72.12	N	23	B	3J	4.1(SE)

DATE	O-TIME GMT	LAT N	LONG W	DEPTH KM	N	Q	G	MAG
1957								
OCT 30	232438.8	7.23	72.53	N	11	D	3M	
NOV 10	102123.7	7.85	74.48	081	29	B	5M	+
NOV 27	032219.0	5.23	72.78	256	10	D	5M	
1958								
MAR 03	171315.8	5.13	73.45	181	12	B	5M	+
MAR 06	054724.4	6.84	73.17	169	07	C	5M	
APR 08	043529.3	6.77	73.29	054	17	B	5M	+
AUG 15	062054.5	6.69	73.03	175	20	A	5M	D(R)
AUG 28	172059.4	8.27	71.20	015	07	D	5M	
SEP 07	024819.2	6.80	73.21	160	12	B	5M	
OCT 18	063413.1	6.79	72.28	N	25	B	3M	5.5(R)
NOV 04	091649.2	6.80	73.10	164	20	B	5M	5.5(R)
NOV 12	060913.6	9.26	69.75	N	25	B	1J	4.4(SE)
NOV 13	090622.0	8.93	69.67	N	24	C	1J	4.5(SE)
NOV 26	141114.9	6.15	73.28	218	09	D	5M	
DEC 09	151339.1	6.29	73.12	209	10	D	5M	
DEC 28	051317.8	9.06	69.78	N	25	C	1J	4.1(SE)
1959								
JAN 13	163249.4	7.01	73.75	134	10	D	5M	
APR 07	102952.1	6.73	73.11	168	08	D	5M	
APR 11	144624.1	6.82	72.15	N	17	C	3M	
APR 15	213517.5	6.79	73.16	175	11	C	5M	
APR 22	172411.5	7.58	72.47	N	19	B	3M	+
MAY 24	000024.1	7.52	71.96	N	07	D	3M	
MAY 28	040657.0	6.75	72.98	168	16	C	5M	+
JUN 15	034839.9	7.23	72.11	N	07	D	3M	
JUN 30	224230.1	8.30	71.23	N	17	C	3J	E(R)
JUL 06	180337.3	6.72	73.52	173	09	C	5M	
JUL 17	225214.3	7.13	72.00	N	19	B	3J	+
JUL 24	130457.7	6.78	72.97	166	09	C	5M	
OCT 16	085326.1	6.69	73.03	178	12	B	5M	
NOV 21	144421.3	6.70	73.06	162	05	C	5M	
1960								
JAN 30	014256.6	6.77	73.14	168	12	B	5M	
FEB 07	042459.5	7.19	72.23	036	23	B	3J	+
FEB 10	225253.3	6.85	72.72	152	11	D	5M	
MAR 06	222650.8	6.88	73.09	162	11	C	5M	
MAR 26	084435.4	6.76	73.07	170	10	B	5M	
JUN 25	135359.9	6.79	73.03	168	32	A	5M	+
JUL 29	092942.9	7.42	71.96	N	15	B	3M	+

DATE	O-TIME GMT	LAT N	LONG W	DEPTH KM	N	Q	G	MAG
1960								
AUG 15	231719.7	6.63	74.15	169	08	D	5M	
AUG 16	225156.6	9.31	72.60	111	08	D	5M	
OCT 20	061242.0	10.63	70.15	N	14	D	1M	
NOV 14	230228.4	6.85	73.15	159	11	C	5M	
NOV 16	153827.2	10.13	74.05	080	15	B	5M	4.4(SE)
NOV 18	073713.1	10.44	73.75	131	06	D	5M	
1961								
JAN 14	161728.4	6.80	73.00	164	26	A	5M	+
FEB 17	061158.8	6.83	73.13	163	14	B	5M	
FEB 27	010753.8	6.72	73.07	171	26	A	5M	+
APR 03	011030.6	6.82	72.89	159	21	B	5M	+
APR 12	113658.0	6.96	73.14	150	10	B	5M	
APR 25	094209.0	8.75	70.85	N	10	C	1M	
MAY 10	085559.2	9.22	71.17	N	09	C	1M	
JUN 15	005133.7	6.79	73.12	157	13	B	5M	
JUN 16	103201.7	8.92	73.44	120	27	B	5M	6.0(GS)
JUN 25	105819.2	11.21	74.68	N	17	B	5M	4.1(SE)
JUN 26	164340.5	11.41	74.57	N	18	B	5M	
JUN 28	180249.9	7.02	73.20	144	09	B	5M	
AUG 26	011940.7	6.85	73.07	160	10	B	5M	
SEP 03	101930.8	6.44	72.95	194	10	D	5M	
SEP 04	162724.6	9.75	70.91	N	07	C	1M	
OCT 26	215619.5	6.81	73.00	170	17	B	5M	+
NOV 13	081223.6	8.68	70.81	N	06	D	1M	
DEC 23	143627.0	6.97	73.10	145	16	B	5M	+
1962								
JAN 01	132442.9	6.87	73.14	153	08	D	5M	
FEB 03	213820.7	6.74	73.07	168	16	C	5M	+
FEB 18	172515.7	8.12	74.86	N	34	B	5M	5.6(SE)
FEB 20	160217.0	6.65	73.03	172	14	B	5M	
MAR 25	152854.4	6.86	73.09	168	11	C	5M	
APR 30	074851.6	6.84	73.09	161	15	A	5M	
MAY 13	091236.6	6.79	72.89	166	24	B	5M	+
JUL 11	135831.8	6.92	73.07	150	11	B	5M	
JUL 30	185752.4	6.80	73.05	164	11	C	5M	
AUG 09	042156.0	6.84	73.03	166	20	B	5M	+
AUG 17	030749.8	7.94	71.53	023	19	B	4J	+
SEP 05	063913.7	6.85	73.02	158	09	B	5M	
OCT 23	090203.2	9.50	70.21	N	16	B	2J	+
NOV 19	143034.6	6.73	72.97	170	24	A	5M	+
1963								
JAN 04	211711.8	6.82	73.13	160	18	B	5M	

DATE	O-TIME GMT	LAT N	LONG W	DEPTH KM	N	Q	G	MAG
1963								
JAN 16	035259.2	6.62	72.94	172	19	C	5M	
FEB 03	125216.9	7.56	72.17	038	26	A	4J	+
FEB 06	032802.2	6.83	73.11	155	25	B	5M	+
FEB 20	145121.1	6.96	73.21	161	11	D	5M	
MAR 02	194202.8	7.08	73.18	204	12	D	5M	
MAR 27	123154.2	6.75	73.02	185	19	B	5M	4.6(CGS)
MAR 27	131537.7	6.75	73.07	175	12	C	5M	
APR 02	005747.0	6.80	73.19	161	17	B	5M	
APR 10	065635.6	6.65	73.01	177	21	C	5M	5.3(CGS)
MAY 02	130528.4	6.97	73.14	148	12	A	5M	
MAY 07	180026.7	12.07	72.11	069	17	B	5M	4.4(CGS)
MAY 13	013241.3	6.86	73.30	160	16	C	5M	4.3(CGS)
MAY 27	180026.7	12.07	72.11	069	17	B	5M	4.4(CGS)
MAY 28	082246.6	6.81	72.86	160	21	B	5M	4.2(CGS)
MAY 30	015647.6	6.89	72.94	153	11	B	5M	3.9(CGS)
JUN 02	222621.5	8.33	74.86	N	21	B	5M	+
JUN 03	113153.7	5.32	72.99	043	32	B	5M	5.5(BCIS)
JUN 08	124607.3	6.90	72.92	160	21	A	5M	4.7(CGS)
JUN 26	142312.1	6.76	73.02	173	24	B	5M	4.5(CGS)
JUN 30	153358.8	6.74	72.95	175	13	B	5M	3.8(CGS)
JUL 08	210258.4	6.72	72.98	167	14	B	5M	4.0(CGS)
JUL 11	141831.1	6.94	73.09	151	10	D	5M	4.0(CGS)
JUL 12	064355.5	6.82	72.99	164	17	B	5M	4.5(CGS)
JUL 25	070424.8	6.79	73.01	165	38	A	5J	5.2(CGS)
SEP 03	183745.9	6.80	73.06	167	26	A	5M	4.4(CGS)
OCT 01	024331.4	6.82	73.02	160	14	A	5M	4.6(CGS)
NOV 13	090113.1	6.93	73.11	149	11	A	5M	4.0(CGS)
NOV 24	164933.2	11.40	73.86	108	12	B	5M	4.1(CGS)
NOV 27	094042.9	6.61	72.89	182	11	C	5M	4.0(CGS)
DEC 10	055225.9	7.68	73.84	004	10	D	5M	3.9(CGS)
DEC 12	205445.3	6.79	72.98	163	27	A	5M	4.9(CGS)
DEC 22	231357.6	6.79	73.01	166	38	A	5J	5.2(CGS)
DEC 23	223426.8	12.42	72.94	046	22	B	5M	4.5(CGS)
1964								
JAN 06	230643.4	6.79	72.95	165	09	A	5M	4.5(CGS)
JAN 25	194849.3	10.01	69.33	N	14	B	2J	4.5(CGS)
JAN 30	011118.4	6.99	72.77	140	11	C	5M	3.9(CGS)
FEB 06	043601.0	6.78	73.03	167	31	A	5M	5.0(CGS)
FEB 14	035714.3	6.40	73.28	207	09	D	5M	4.0(CGS)
FEB 26	123125.7	6.70	73.15	177	10	C	5M	4.1(CGS)
FEB 29	140501.4	6.87	73.02	161	16	B	5M	4.4(CGS)
MAR 13	081352.0	8.92	69.77	N	12	C	2M	4.1(CGS)

DATE	O-TIME GMT	LAT N	LONG W	DEPTH KM	N	Q	G	MAG
1964								
MAR 18	015208.6	6.78	73.19	143	12	D	5M	3.9(CGS)
MAR 25	034509.1	6.84	72.99	168	10	C	5M	3.7(CGS)
MAY 12	004711.8	6.89	73.05	156	09	D	5M	4.0(CGS)
MAY 16	054013.8	6.83	73.03	161	15	B	5M	4.4(CGS)
MAY 27	110626.5	6.82	72.97	168	32	A	5M	5.0(CGS)
JUN 03	122921.1	10.48	70.86	N	05	B	2M	4.1(CGS)
JUN 08	104803.0	9.12	72.48	213	14	B	5M	4.5(CGS)
JUN 13	184306.9	6.79	72.97	170	09	C	5M	4.3(CGS)
JUN 23	195322.4	6.83	72.98	165	12	B	5M	4.3(CGS)
JUL 28	213715.9	6.84	72.98	170	17	B	5M	5.0(CGS)
AUG 09	153108.9	5.76	72.98	006	10	B	5M	4.0(CGS)
AUG 15	212203.6	6.80	72.99	170	16	A	5M	4.8(CGS)
AUG 23	122340.1	6.84	72.96	169	13	B	5M	4.2(CGS)
SEP 02	175005.9	8.27	72.80	N	10	B	4M	4.1(CGS)
SEP 02	181215.8	8.08	72.78	026	29	A	4J	4.8(CGS)
SEP 03	041616.6	8.24	72.81	N	07	C	4M	
SEP 03	113623.2	6.83	73.01	162	16	A	5M	4.8(CGS)
SEP 10	023929.4	7.39	73.05	153	13	B	5M	4.4(ISC)
SEP 22	094631.2	10.55	69.91	N	14	A	2J	4.1(CGS)
OCT 01	035016.0	7.19	72.11	N	10	C	4J	4.0(CGS)
OCT 09	192642.4	6.81	72.99	167	34	A	5J	5.3(CGS)
OCT 14	220957.6	10.46	72.70	068	11	C	5M	3.7(CGS)
OCT 30	164756.4	6.78	72.98	168	24	A	5M	4.5(CGS)
NOV 26	045034.5	6.26	72.70	205	12	B	5M	3.9(CGS)
NOV 29	091106.5	6.81	73.13	161	31	A	5M	4.9(CGS)
DEC 15	015840.5	8.47	71.69	032	23	B	4J	5.3(CGS)
DEC 15	082423.6	6.79	73.05	165	15	A	5M	4.4(ISC)
DEC 18	220736.6	6.91	73.07	158	15	B	5M	4.0(CGS)
1965								
JAN 07	113933.2	10.41	69.55	N	13	C	2M	5.3(CGS)
JAN 14	121901.4	6.82	73.01	163	12	A	5M	4.9(CGS)
JAN 24	011934.8	6.80	73.04	173	29	A	5J	5.4(CGS)
FEB 14	065152.4	6.72	73.05	176	08	B	5M	4.2(ISC)
FEB 26	233615.4	6.82	73.01	164	40	A	5J	5.7(CGS)
MAR 22	094609.2	6.87	72.97	159	23	A	5M	4.9(CGS)
APR 04	043331.5	6.90	72.74	157	12	D	5M	4.0(ISC)
APR 15	012150.0	6.80	73.04	168	13	B	5M	5.0(CGS)
APR 22	013954.7	6.88	73.04	161	09	B	5M	4.5(ISC)
MAY 01	163541.2	6.74	72.82	167	12	B	5M	4.9(CGS)
MAY 10	035234.4	6.89	73.05	158	11	B	5M	3.9(CGS)
MAY 16	053840.0	6.76	72.95	169	06	D	5M	4.0(CGS)
MAY 16	195354.0	6.38	72.71	202	06	D	5M	3.9(ISC)

DATE	O-TIME GMT	LAT N	LONG W	DEPTH KM	N	Q	G	MAG
1965								
MAY 20	175228.9	6.71	73.08	164	11	C	5M	4.3(CGS)
MAY 21	225801.0	5.38	73.10	273	07	D	5M	3.6(CGS)
MAY 23	231103.3	11.91	70.26	N	05	D	2M	4.7(CGS)
JUN 01	151100.6	7.03	73.45	151	12	D	5M	4.2(CGS)
JUN 19	180054.7	6.24	73.41	167	09	D	5M	5.0(CGS)
JUN 21	092756.8	6.72	73.05	174	14	A	5M	4.1(CGS)
JUN 26	095645.0	6.77	72.97	168	08	A	5M	4.3(CGS)
JUN 27	125546.0	6.73	72.96	173	10	A	5M	4.7(CGS)
JUN 28	062012.9	6.73	72.98	168	11	A	5M	4.4(CGS)
JUN 29	200017.7	6.62	72.92	180	13	D	5M	4.8(CGS)
JUL 19	041321.2	9.20	70.28	020	42	A	S	5.3(CGS)
JUL 26	110121.6	6.91	72.91	179	12	C	5M	4.8(CGS)
JUL 30	072010.8	6.80	73.01	162	42	A	5J	5.5(CGS)
AUG 09	153108.6	5.71	72.94	007	10	C	5M	4.0(CGS)
AUG 11	194127.6	6.69	72.93	178	10	B	5M	4.6(CGS)
AUG 11	200417.4	6.73	72.94	175	11	D	5M	4.9(CGS)
SEP 10	122952.0	9.92	70.84	N	28	A	2J	4.9(CGS)
SEP 11	221518.5	6.92	71.81	N	20	A	4J	4.4(CGS)
SEP 15	083934.9	6.80	73.05	165	07	A	5M	4.4(CGS)
SEP 19	232419.2	9.90	70.26	N	17	B	2J	5.0(CGS)
SEP 22	203529.9	7.04	72.83	142	10	D	5M	3.8(CGS)
SEP 26	184937.6	9.17	73.97	N	10	D	5M	3.8(CGS)
OCT 09	164946.2	6.62	72.89	177	08	C	5M	4.6(CGS)
OCT 15	074823.2	6.73	72.93	171	06	C	5M	4.2(CGS)
OCT 17	104121.2	6.94	73.43	157	11	D	5M	4.2(CGS)
OCT 19	232257.2	6.82	73.01	166	08	B	5M	4.3(CGS)
OCT 20	115334.8	6.82	73.03	158	17	A	5M	5.1(CGS)
NOV 06	051826.7	6.54	73.06	196	10	D	5M	4.3(CGS)
NOV 08	142413.5	6.92	73.03	161	08	D	5M	4.1(CGS)
NOV 23	054753.5	6.97	72.99	143	10	D	5M	3.4(CGS)
NOV 25	232949.0	6.86	73.10	154	11	A	5M	4.6(CGS)
NOV 30	091613.8	6.83	73.00	162	16	A	5M	4.7(CGS)
DEC 03	184828.1	6.44	72.77	201	06	D	5M	4.7(CGS)
DEC 12	183434.5	6.79	73.09	165	11	A	5M	4.6(CGS)
DEC 17	211343.8	6.84	73.03	166	13	A	5M	4.6(CGS)
DEC 21	122546.5	6.80	73.03	188	15	C	5M	4.9(CGS)
DEC 24	225127.0	6.82	73.05	161	06	A	5M	4.3(CGS)
1966								
JAN 06	042000.7	6.79	73.01	164	34	A	5J	5.3(CGS)
JAN 10	111306.5	7.53	72.15	055	28	A	4J	4.9(CGS)
JAN 24	094204.4	6.83	73.03	161	11	A	5M	4.5(CGS)
JAN 29	032944.8	6.62	72.88	183	06	D	5M	3.4(CGS)

DATE	O-TIME GMT	LAT N	LONG W	DEPTH KM	N	Q	G	MAG
1966								
JAN 29	165340.0	6.69	72.91	173	07	D	5M	4.8(CGS)
JAN 30	031745.2	6.80	73.10	167	11	B	5M	5.1(CGS)
FEB 01	090757.7	6.35	72.84	206	06	D	5M	3.9(CGS)
FEB 09	011924.6	6.91	73.02	152	09	A	5M	4.5(CGS)
FEB 14	110526.5	11.61	72.20	N	07	D	2M	3.8(CGS)
FEB 20	041029.8	6.87	73.04	157	16	A	5M	4.8(CGS)
FEB 24	173449.4	6.72	73.12	062	10	B	5M	4.5(CGS)
FEB 25	100633.0	6.82	72.97	164	11	D	5M	4.0(CGS)
MAR 05	022920.0	9.93	69.32	N	20	B	2J	4.8(CGS)
MAR 05	143328.2	8.11	74.72	083	23	B	5M	4.8(CGS)
MAR 06	210421.4	7.06	71.70	042	19	A	4J	4.6(CGS)
MAR 09	102446.3	6.87	73.02	156	09	D	5M	4.3(CGS)
MAR 18	045929.1	6.82	73.02	161	05	C	5M	4.5(CGS)
MAR 26	021411.9	6.78	73.10	163	18	B	5M	4.6(CGS)
MAR 29	093220.5	7.15	73.24	124	07	D	5M	3.8(CGS)
MAR 29	100615.7	7.66	73.90	159	09	D	5M	4.1(CGS)
APR 02	181658.0	6.84	73.09	162	17	B	5M	5.1(CGS)
APR 09	154956.8	6.74	72.96	168	10	B	5M	5.2(ISC)
APR 10	103337.6	6.81	73.00	166	41	A	5J	5.1(CGS)
APR 21	081827.1	6.87	73.00	167	12	B	5M	4.8(CGS)
APR 21	180957.3	6.75	73.23	171	08	B	5M	3.8(CGS)
APR 29	064522.4	6.83	73.06	159	08	C	5M	4.3(CGS)
APR 30	012758.5	6.74	73.15	178	08	D	5M	3.5(CGS)
MAY 18	040003.0	6.20	73.61	145	07	B	5M	3.7(CGS)
MAY 23	060606.5	6.87	73.20	159	13	C	5M	4.1(CGS)
MAY 27	051222.1	6.77	73.00	169	14	B	5M	4.4(CGS)
JUN 12	035624.2	6.40	72.96	172	11	B	5M	4.9(CGS)
JUN 20	075701.3	11.02	69.52	N	28	B	2J	4.5(CGS)
JUN 24	200011.3	6.85	73.06	168	16	A	5M	4.8(CGS)
JUL 01	063313.2	7.00	73.17	147	09	D	5M	3.9(CGS)
JUL 07	001033.4	6.80	72.99	162	14	A	5M	4.8(CGS)
JUL 11	072819.1	6.83	73.02	161	10	A	5M	4.6(CGS)
JUL 11	092957.0	6.80	73.32	165	08	D	5M	4.7(CGS)
JUL 15	053548.2	6.77	72.96	170	06	D	5M	4.2(CGS)
JUL 26	110124.4	7.43	72.97	173	08	D	5M	4.8(CGS)
AUG 07	082102.0	6.80	73.02	168	15	A	5M	4.6(CGS)
SEP 06	162130.1	6.64	72.88	180	08	B	5M	4.1(CGS)
SEP 09	184001.7	10.87	69.38	N	32	A	2J	5.0(CGS)
SEP 11	032054.9	6.80	73.00	163	22	A	5M	4.7(CGS)
SEP 11	173805.7	6.83	72.97	162	39	A	5J	5.9(CGS)
OCT 22	074549.2	9.83	70.91	N	12	B	2M	4.5(CGS)
OCT 22	074902.4	9.84	70.79	N	05	B	2M	
NOV 27	011040.2	6.87	73.02	158	13	B	5M	4.4(CGS)

DATE	O-TIME GMT	LAT N	LONG W	DEPTH KM	N	Q	G	MAG
1967								
JAN 03	172144.0	6.76	73.01	168	20	A	5M	4.4(CGS)
JAN 15	180319.8	6.95	73.11	150	09	D	5M	4.1(CGS)
JAN 22	081816.9	6.77	72.96	169	22	A	5M	4.6(CGS)
JAN 23	092750.3	6.85	73.02	163	10	B	5M	4.2(CGS)
JAN 25	093307.4	7.01	72.77	135	13	C	5M	4.0(CGS)
FEB 05	124901.9	8.17	71.08	042	14	B	4J	4.4(CGS)
FEB 05	170229.6	6.84	73.06	164	08	D	5M	4.0(CGS)
FEB 25	123025.1	6.86	73.11	160	10	D	5M	4.3(CGS)
FEB 27	065053.1	6.73	73.11	180	11	D	5M	4.1(CGS)
MAR 07	090309.2	6.84	73.07	163	09	A	5M	4.4(CGS)
MAR 09	004157.4	6.81	73.05	161	09	A	5M	4.5(CGS)
MAR 11	135602.1	10.84	69.69	N	05	C	2M	3.9(CGS)
MAR 19	212926.3	6.83	73.13	158	11	A	5M	4.3(CGS)
MAR 20	225140.7	7.39	71.96	N	11	A	4M	4.2(CGS)
MAR 21	181145.3	6.79	73.00	162	38	A	5J	5.4(CGS)
APR 14	094825.8	6.77	73.02	166	10	B	5M	4.3(CGS)
MAY 04	070301.5	6.78	73.09	166	17	A	5M	4.5(CGS)
MAY 08	080628.6	6.66	73.48	N	26	A	4M	4.5(CGS)
MAY 11	060820.6	6.82	73.04	165	23	A	5M	4.9(CGS)
MAY 12	092848.8	6.86	73.04	162	18	A	5M	4.6(CGS)
MAY 19	070004.6	7.12	71.97	N	09	A	4M	
MAY 20	120932.5	6.97	72.96	146	09	A	5M	4.3(CGS)
JUN 11	052003.5	9.56	70.81	N	10	A	2M	4.2(CGS)
JUN 14	114321.6	6.83	72.85	155	08	D	5M	3.8(CGS)
JUN 18	022607.8	6.81	73.03	162	16	A	5M	4.4(CGS)
JUL 02	164818.9	6.83	72.98	166	10	B	5M	3.9(CGS)
JUL 05	101915.1	6.48	73.03	179	09	D	5M	3.8(CGS)
JUL 06	213646.9	6.62	73.07	151	11	B	5M	4.3(CGS)
JUL 14	003258.1	6.81	72.97	163	11	A	5M	4.4(CGS)
JUL 26	090739.7	8.57	70.96	N	29	B	2J	4.6(CGS)
JUL 29	102426.5	6.83	73.01	165	44	A	5J	6.0(CGS)
AUG 05	214653.9	6.79	73.04	164	14	A	5M	4.0(CGS)
AUG 14	144625.2	6.89	73.08	160	09	A	5M	4.0(CGS)
AUG 15	040658.6	6.77	73.06	170	19	B	5M	4.5(CGS)
AUG 19	070310.9	6.84	73.03	161	21	A	5M	4.6(CGS)
AUG 25	060123.5	6.83	72.96	171	11	B	5M	4.2(CGS)
SEP 01	024922.2	6.76	73.11	170	17	A	5M	4.6(CGS)
SEP 03	143236.3	6.78	73.15	141	09	D	5M	4.1(CGS)
SEP 03	170203.7	6.76	73.39	109	07	D	5M	4.0(CGS)
OCT 09	024514.5	6.79	73.06	199	11	C	5M	4.2(CGS)
OCT 21	174538.3	6.82	73.03	163	14	A	5M	4.4(CGS)
OCT 25	044940.7	6.83	72.98	172	22	A	5M	4.7(CGS)
OCT 31	050423.3	7.57	72.99	171	15	B	5M	4.2(CGS)

DATE	O-TIME GMT	LAT N	LONG W	DEPTH KM	N	Q	G	MAG
1967								
NOV 30	222245.4	6.84	73.02	161	09	B	5M	4.2(CGS)
DEC 07	081701.4	9.67	70.21	N	20	B	2J	4.3(CGS)
DEC 21	113724.5	7.04	72.02	029	30	A	4J	5.4(CGS)
DEC 28	173341.6	6.95	72.85	196	32	A	5J	5.2(CGS)
1968								
JAN 11	071214.2	6.81	73.02	161	09	A	5M	4.0(CGS)
JAN 15	043554.2	6.80	72.96	165	18	A	5M	4.7(CGS)
JAN 30	043918.0	6.76	73.03	171	22	A	5M	5.0(CGS)
MAR 01	183508.6	6.85	73.04	160	11	A	5M	4.4(CGS)
MAR 16	174950.8	6.74	73.00	170	07	D	5M	4.1(CGS)
MAR 23	164912.4	6.75	73.04	167	16	A	5M	4.4(CGS)
APR 04	184642.3	6.87	73.05	163	13	B	5M	4.3(CGS)
APR 14	142457.4	6.78	73.00	165	31	A	5M	5.0(CGS)
APR 25	235235.9	6.81	72.99	160	17	A	5M	4.3(CGS)
MAY 04	011924.1	6.75	73.11	170	14	A	5M	4.4(CGS)
MAY 07	090030.3	6.80	72.99	162	45	A	S	5.7(CGS)
MAY 13	193605.8	9.00	71.06	N	29	A	2J	4.8(CGS)
MAY 24	234707.0	10.85	69.35	N	11	B	2M	4.8(CGS)
JUN 16	091359.7	6.74	73.10	207	13	B	5M	4.1(CGS)
JUN 17	014611.3	6.49	72.98	170	05	D	5M	4.0(CGS)
JUL 03	081923.0	9.68	70.25	N	07	D	2M	4.0(CGS)
JUL 03	183945.9	6.83	73.07	158	07	A	5M	3.8(CGS)
JUL 21	042811.5	6.74	72.96	171	07	C	5M	4.0(CGS)
JUL 24	132530.0	6.62	73.40	187	11	B	5M	4.0(CGS)
JUL 26	182955.8	6.79	72.98	166	20	A	5M	4.6(CGS)
AUG 12	005034.5	6.64	73.23	264	10	C	5M	3.8(CGS)
AUG 29	211547.1	6.79	73.04	167	09	B	5M	4.6(CGS)
SEP 02	034003.3	10.89	69.43	N	08	C	2M	4.1(CGS)
OCT 08	102824.3	6.46	73.84	186	06	D	5M	3.8(CGS)
OCT 12	021958.2	6.79	73.05	171	20	B	5M	4.6(CGS)
OCT 22	054914.6	6.80	72.98	161	05	A	5M	4.1(CGS)
OCT 22	163132.5	6.84	72.97	176	14	B	5M	4.5(CGS)
OCT 27	001934.2	11.53	72.62	090	23	B	5M	4.5(CGS)
NOV 10	133737.1	6.79	73.05	162	16	B	5M	4.4(CGS)
NOV 15	092828.5	6.65	72.94	179	10	B	5M	4.0(CGS)
NOV 17	001610.1	9.55	72.60	175	38	A	5M	5.7(CGS)
NOV 18	150907.7	6.77	72.99	166	09	C	5M	4.2(CGS)
DEC 01	151640.2	6.84	73.03	162	21	A	5J	5.1(CGS)
DEC 02	121131.8	6.70	72.94	172	09	B	5M	4.1(CGS)
DEC 08	010422.8	6.03	72.27	089	16	D	5M	4.4(CGS)
DEC 10	063642.6	6.80	73.14	169	09	C	5M	4.2(CGS)
DEC 30	094413.4	6.86	72.94	176	06	A	5M	3.8(CGS)

DATE	O-TIME GMT	LAT N	LONG W	DEPTH KM	N	Q	G	MAG
1969								
JAN 26	114928.5	6.63	72.98	185	09	C	5M	4.3(CGS)
FEB 07	131900.6	6.31	73.03	155	08	C	5M	4.1(CGS)
FEB 08	074009.3	6.62	73.04	185	10	C	5M	4.1(CGS)
FEB 24	224417.0	6.81	73.00	162	36	A	5M	5.0(CGS)
APR 18	190519.9	6.80	72.96	166	12	A	5M	4.6(CGS)
APR 19	144555.6	6.82	73.04	161	06	B	5M	4.1(CGS)
MAY 29	224905.8	7.38	73.04	158	08	A	5M	4.0(CGS)
JUN 22	081729.3	6.75	72.93	176	13	B	5M	4.1(CGS)
JUL 04	071224.3	6.81	73.02	173	10	B	5M	3.9(CGS)
JUL 14	054446.9	6.79	73.03	167	18	A	5M	4.6(CGS)
JUL 16	221250.6	6.87	73.06	161	08	D	5M	4.3(CGS)
JUL 19	122849.2	6.78	73.07	168	20	A	5M	4.7(CGS)
AUG 15	143537.9	6.80	73.06	169	12	B	5M	4.5(CGS)
AUG 16	184238.6	11.35	72.40	N	06	D	5M	3.6(CGS)
AUG 23	143537.3	6.83	73.02	170	14	C	5M	4.6(CGS)
SEP 10	124124.0	8.53	74.02	110	12	C	5M	4.4(CGS)
SEP 23	143745.9	6.84	72.98	167	13	A	5M	3.8(CGS)
OCT 17	134629.9	6.87	73.04	158	09	B	5M	4.0(CGS)
OCT 20	131132.2	10.90	72.30	N	31	A	5M	5.1(CGS)
OCT 20	131137.6	10.93	72.46	N	14	B	5M	5.7(CGS)
NOV 09	122628.0	6.84	73.00	165	17	A	5M	4.6(CGS)
1970								
JAN 01	112104.5	9.12	69.75	N	13	C	2J	4.1(CGS)
JAN 10	115639.9	6.85	73.05	159	13	A	5M	4.6(CGS)
JAN 27	092948.7	7.54	71.95	049	30	A	4J	5.7(CGS)
FEB 26	065821.6	6.77	73.10	171	12	A	5M	4.4(CGS)
MAR 12	112159.0	6.72	73.01	169	11	B	5M	4.6(CGS)
APR 04	004248.9	6.84	72.93	168	11	B	5M	4.4(CGS)
APR 10	040324.4	6.78	73.01	168	19	A	5M	4.6(CGS)
MAY 19	102259.4	10.89	68.93	N	29	A	2J	5.1(CGS)
JUN 08	031926.6	10.86	68.95	N	22	A	2J	4.7(CGS)
JUN 08	164329.7	6.77	72.96	172	10	B	5M	4.5(CGS)
JUN 14	083626.1	6.78	73.08	162	15	B	5M	4.8(CGS)
JUN 22	015214.0	6.76	73.04	169	15	B	5M	4.5(CGS)
JUL 04	153309.6	6.88	72.91	168	09	C	5M	4.3(CGS)
JUL 20	174459.5	6.82	73.00	161	20	A	5M	5.0(CGS)
AUG 29	025945.6	7.57	71.95	N	28	A	S	4.6(CGS)
SEP 04	023336.7	6.77	72.98	166	06	C	5M	4.2(CGS)
SEP 12	180702.2	9.35	74.17	139	08	D	5M	4.9(CGS)
SEP 19	020447.7	10.69	73.15	111	17	B	5M	4.9(CGS)
OCT 10	155726.5	9.14	70.20	N	10	B	2M	4.7(CGS)
OCT 17	034125.9	6.79	73.02	167	18	A	5J	4.5(CGS)

DATE	O-TIME GMT	LAT N	LONG W	DEPTH KM	N	Q	G	MAG
1970								
OCT 26	105428.9	6.88	74.42	043	10	D	SM	4.4(GGS)
NOV 12	001055.1	6.71	73.03	172	16	B	SM	4.5(GGS)
DEC 14	040633.2	9.96	72.63	179	33	A	SM	5.2(GGS)

APPENDIX 2

P-WAVE RADIATION PATTERNS FOR EARTHQUAKES IN WESTERN VENEZUELA AND NORTHERN COLOMBIA

Large symbols represent all WWSSN stations the records of which were read personally by the author and the first motions of which at the time of reading the record, were judged unambiguous. Most readings were made on short-period seismograms. Small symbols represent first motions read by others and reported in bulletins. These have been used only for the earthquakes of April 21, 1957, and December 21, 1967.

All plots are made on equal-area projections of the lower hemisphere of the focal sphere. Take-off angles for the seismic ray paths from the focus to station were taken from Ritsema (1958). For shallow earthquakes (depth < 70 km), a critical angle of 57° was assumed for the angle at which P_n waves leave the focal sphere.

Hachured regions were determined by the computer program of Dillinger *et al.* (1971) and represent variations of positions of the poles of the nodal planes which are permissible under the constraint that the number of inconsistent *P*-wave readings be a minimum. The nodal planes are assumed to be orthogonal. For some earthquakes, the hachured regions indicate a wide range of pairs of nodal planes which are possible with the observed *P* first motions. In these cases, dots indicate those nodal planes which were discussed in the text as being consistent with certain tectonic hypotheses. However, focal mechanisms are plotted on plate A only if the hachured regions indicate that the observed *P*-wave first motions require the plotted mechanism.

The following symbols are applicable to all focal mechanisms:

△△ Compression
○○ Dilatation
P Axis of maximum pressure (Honda, 1962)
T Axis of maximum tension.

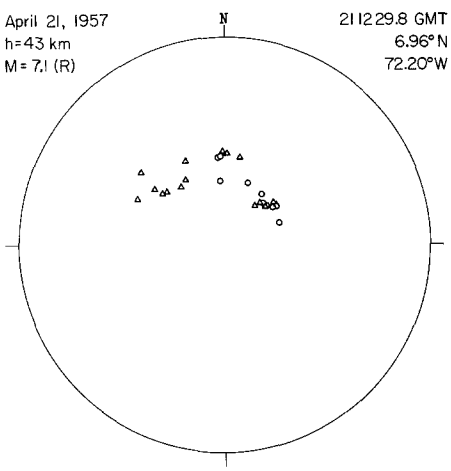
April 21, 1957
h=43 km
M=7.1 (R)
N
211229.8 GMT
6.96°N
72.20°W

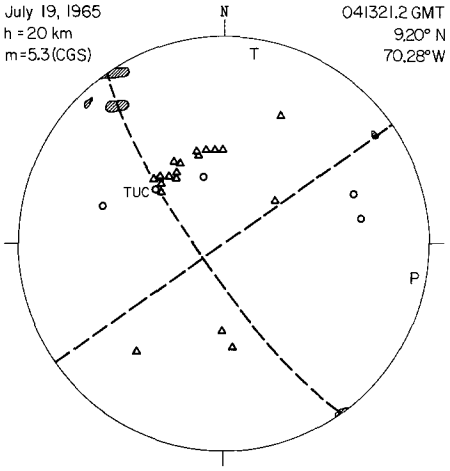
July 19, 1965
h=20 km
m=5.3(CGS)
N
T
TUC
P
041321.2 GMT
9.20° N
70.28°W

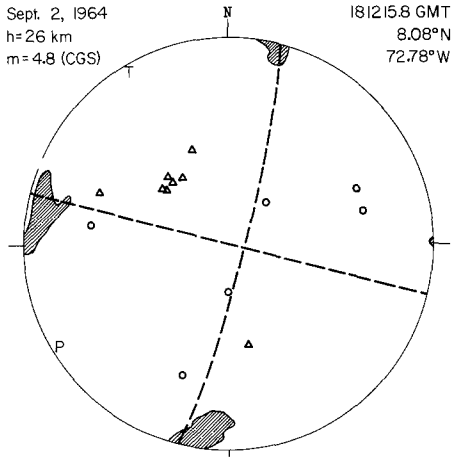
Sept. 2, 1964
h=26 km
m=4.8 (CGS)
N
T
P
181215.8 GMT
8.08°N
72.78°W

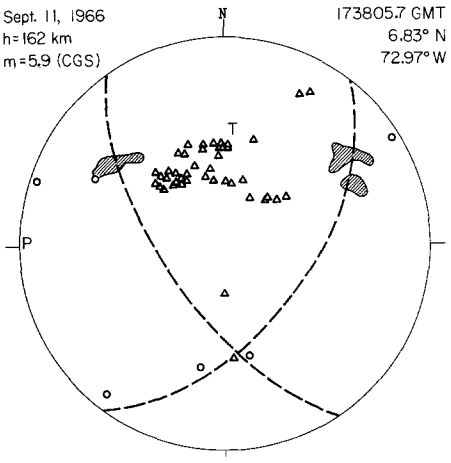
Sept. 11, 1966
h=162 km
m=5.9 (CGS)
N
T
P
173805.7 GMT
6.83° N
72.97° W

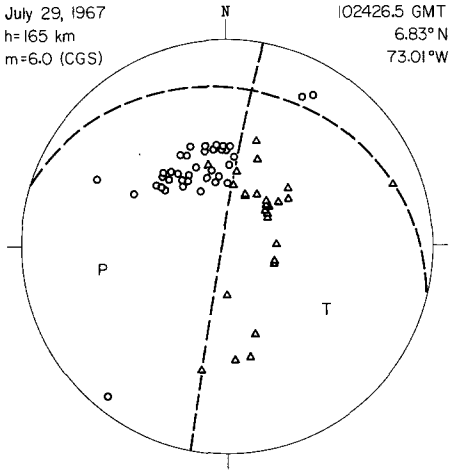
July 29, 1967
h=165 km
m=6.0 (CGS)
N
102426.5 GMT
6.83° N
73.01°W
P
T

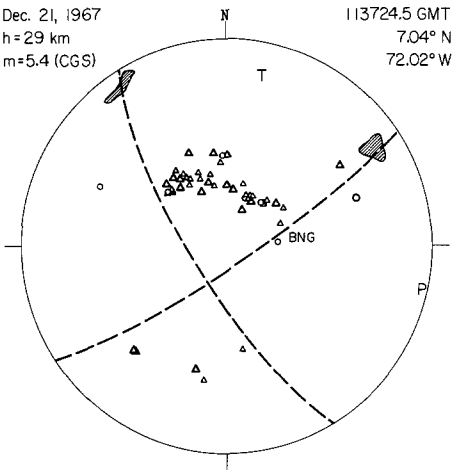
Dec. 21, 1967
h=29 km
m=5.4 (CGS)
N
113724.5 GMT
7.04° N
72.02° W
T
BNG
P

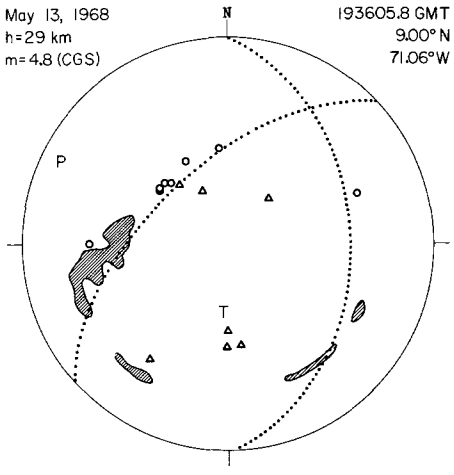
May 13, 1968
h=29 km
m=4.8 (CGS)
N
193605.8 GMT
9.00° N
71.06°W
P
T

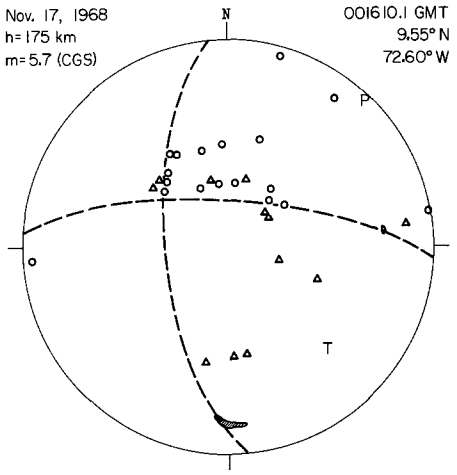
Nov. 17, 1968
h=175 km
m=5.7 (CGS)
N
001610.1 GMT
9.55° N
72.60° W
P
T

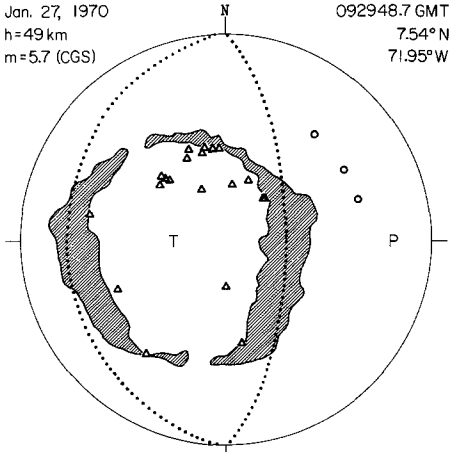
Jan. 27, 1970
h=49 km
m=5.7 (CGS)
N
092948.7 GMT
7.54° N
71.95°W
T
P

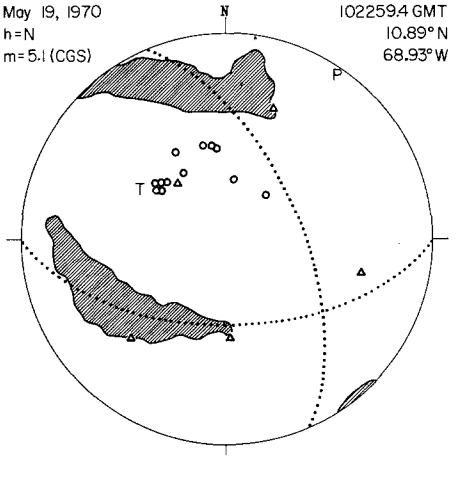
May 19, 1970
h=N
m=5.1 (CGS)
N
102259.4 GMT
10.89° N
68.93° W
P
T

References

Allen, C. R. (1968). The tectonic environments of seismically active and inactive areas along the San Andreas Fault system: *Stanford Univ. Publ., Univ. Ser. Geol. Sci.* **11,** 70–82.

Bolt, B. A. (1960). The revision of earthquake epicenters, focal depths, and origin times using a high-speed computer, *Geophys. J.* **3,** 433–440.

Bolt, B. A., C. Lomnitz, and T. V. McEvilly (1968). Seismological evidence on the tectonics of central and northern California and the Mendocino escarpment, *Bull. Seism. Soc. Am.* **58,** 1725–1767.

Bucher, W. H. (1952). Geologic structure and orogenic history of Venezuela, *Mem. Geol. Soc. Am. 49,* 113 pp.

Case, J. E., L. G. Duran S., A. Lopez R., W. R. Moore (1971). Tectonic investigations in western Colombia and eastern Panama, *Bull. Geol. Soc. Am.* **82,** 2685–2712.

Centeno-Grau, M. (1940). *Estudios Sismologicos,* Litografia del Comercio, Caracas.

Dewey, J. W. (1971). Seismicity studies with the method of joint hypocenter determination, *Ph.D. Dissertation,* University of California, Berkeley.

Dillinger, W. H., A. J. Pope, and S. T. Harding (1971). The determination of focal mechanisms using *P*- and *S*-wave data, *NOAA Technical Report, NOS, 44.*

Douglas, A. (1967). Joint epicenter determination, *Nature* **215,** 47–48.

Fiedler, G. (1961). Areas afectados por terremotos en Venezuela, *Bol. Geol., Congr. Geol. 3rd, Venezolano* **4,** 1791–1810.

Flinn, E. A. (1965). Confidence regions and error determinations for seismic event location, *Rev. Geophys.* **3,** 157–185.

Freeland, G. L. and R. S. Dietz (1971). Plate tectonic evolution of Caribbean-Gulf of Mexico region, *Nature* **232,** 20–23.

Gutenberg, B. and C. F. Richter (1954). *Seismicity of the Earth and Associated Phenomena,* Princeton.

Herrin, E. (Chairman) *et al.* (1968). 1968 seismological tables for *P* phases, *Bull. Seism. Soc. Am.* **58,** 1193–1352.

Honda, H. (1962). Earthquake mechanism and seismic waves, *Geophys. Notes, Fac. Sci., Tokyo* **15** (supplement).

Isacks, B. and P. Molnar (1969). Mantle earthquake mechanisms and the sinking of the lithosphere, *Nature* **223,** 1121–1124.

Isacks, B. and P. Molnar (1971). Distribution of stresses in the descending lithosphere from a global survey of focal-mechanism solutions of mantle earthquakes, *Rev. Geophys. Space Phys.* **9,** 103–174.

Isacks, B., J. Oliver, and L. R. Sykes (1968). Seismology and the new global tectonics, *J. Geophys. Res.* **73,** 5855–5899.

King, P. B. (compiler) (1969). *Tectonic Map of North America,* U.S. Geological Survey, Washington, D.C.

Mencher, E. (1963). Tectonic history of Venezuela, in *Backbone of the Americas, Am. Assoc. Petrol. Geol. Mem. 2,* 73–87.

Molnar, P. and L. R. Sykes (1969). Tectonics of the Caribbean and middle America regions from focal mechanisms and seismicity, *Bull. Geol. Soc. Am.* **80,** 1639–1684.

Page, R. (1968). Focal depths of aftershocks, *J. Geophys. Res.* **73,** 3897–3903.

Raasveldt, H. C. (1956). Fallas de rumbo en el nordeste de Colombia, *Rev. Petrol., Bogota* **7,** 19–26.

Ramirez, J. E. (1933). Earthquake history of Colombia, *Bull. Seism. Soc. Am.* **23,** 13–22.

Richter, C. F. (1958). *Elementary Seismology,* Freeman, San Francisco.

Ritsema, A. R. (1958). (*i*, Δ)-curves for bodily seismic waves of any focal depth, *Verhandel. 54,* Lembaga Meteorologi dan Geofisik, Djakarta.

Rod, E. (1956). Strike-slip faults of northern Venezuela, *Bull. Am. Assoc. Petrol. Geol.* **40,** 457–476.

Rod, E., C. Jefferson, E. Von der Osten, and R. Mullen (1958). Roundtable discussion—the determination of the Boconó Fault, *Bol. Inform., Asoc. Ven. Geol. Mina y Petroleo.* **1,** 69–100.

Santo, T. (1969). Characteristics of seismicity in South America, *Bull. Earthquake Res. Inst., Tokyo Univ.* **47,** 635–672.

Sbar, M. L., J. M. W. Rynn, F. J. Gumper, and J. C. Lahr (1970). An earthquake sequence and focal mechanism solution, Lake Hopatcong, northern New Jersey, *Bull. Seism. Soc. Am.* **60,** 1231–1243.

Scheffé, H. (1959). *The Analysis of Variance,* Wiley, New York.

Schubert, C. (1969). Geologic structure of a part of the Barinas Mountain Front, Venezuelan Andes, *Bull. Geol. Soc. Am.* **80,** 443–458.

Schubert, C. and R. S. Sifontes (1970). Boconó Fault, Venezuelan Andes: evidence of postglacial movement, *Science* **170,** 66–69.

Sykes, L. R. and M. Ewing (1965). The seismicity of the Caribbean region, *J. Geophys. Res.* **70,** 5065–5074.

Tryggvason, E. and J. E. Lawson (1970). The intermediate earthquake source near Bucaramanga, Colombia, *Bull. Seism. Soc. Am.* **60**, 269–276.

SEISMOGRAPHIC STATION
UNIVERSITY OF CALIFORNIA
BERKELEY, CALIFORNIA 94720

Manuscript received May 25, 1972

CARIBBEAN SEA

LAKE MARACAIBO

LGN

LCV

UAV

BLV

VEN.
COL.

74°W 73° 72° 71° 70° 69° 68°W

13°N 12° 11° 10° 9° 8° 7° 6°N

SEISMICITY OF NORTHWESTERN VENEZUELA 1930-1970

QUALITY

A	B	C	
● ▲	◐ ▲	○ △	$m_b < 5.0$
● ▲	◐ ▲	○	$5.0 \leq m_b < 6.0$
● ▲	◐ ▲	○	$6.0 \leq m_b$

(Earthquakes deeper than 70km are indicated by triangles; depths are indicated next to quality A and B intermediate-depth epicenters; only quality A intermediate-depth epicenters are plotted in 6.3°N - 7.3°N, 72.5°W - 73.5°W)

E Identified source regions of small earthquakes, southern Cord. de Mérida

Boconó fault zone (Rod et. al. 1958)

Mountain front

Geologic faults (abstracted from King, 1969)

Faulting inferred from strike-slip focal mechanism

Direction of maximum compressional stress inferred from thrust fault focal mechanism

100 km

Plate A in "Seismicity and Tectonis of Western Venezuela," compiled by James W. Dewey. *Bulletin of the Seismologica Society of America*, Vol. 62, No. 6, December 1972.